



Cite this: *Dalton Trans.*, 2016, **45**, 6183

Variable coordination modes and catalytic dehydrogenation of *B*-phenyl amine–boranes†

Amit Kumar, Isobel K. Priest, Thomas N. Hooper* and Andrew S. Weller*

The chemistry of *N*-substituted amine–boranes and their reactivity towards transition metal centres is well established but the chemistry of *B*-substituted amine–boranes is not. Here we present the coordination chemistry of $\text{H}_2\text{PhB}\cdot\text{NMe}_3$ towards a range of Rh(I) fragments with different P–Rh–P ligand bite angles, $\{\text{Rh}(\text{P}^i\text{Pr}_3)_2\}^+$, $\{\text{Rh}(\text{P}^t\text{Bu}_3)_2\}^+$, $\{\text{Rh}(\text{Pr}_2\text{P}(\text{CH}_2)_3\text{P}^i\text{Pr}_2)\}^+$, $\{\text{Rh}(\text{Ph}_2\text{P}(\text{CH}_2)_n\text{PPh}_2)\}^+$ ($n = 3, 5$), as characterised by NMR spectroscopy and single-crystal X-ray diffraction. This reveals a difference in the coordination mode of the amine–borane, with large bite angle fragments favouring η^2 -coordination through a sigma-interaction with BH_2 , whereas fragments with small bite angles favour η^6 -coordination through the aryl group of the amine–borane. The catalytic dehydrocoupling of $\text{H}_2\text{PhB}\cdot\text{NMe}_2\text{H}$ is also explored, with the aminoborane $\text{HPhB}=\text{NMe}_2$ found to be the sole dehydrogenation product. Stoichiometric reactivity with $\text{H}_2\text{PhB}\cdot\text{NMe}_2\text{H}$ again showed small bite angle fragments to prefer η^6 -aryl coordination, while the larger bite angle $\{\text{Rh}(\text{P}^i\text{Pr}_3)_2\}^+$ gave rapid dehydrogenation to form a mixture of the Rh(III) dihydride $[\text{Rh}(\text{P}^i\text{Pr}_3)_2(\text{H})_2(\eta^2\text{-H}_2\text{PhB}\cdot\text{NMe}_2\text{H})][\text{BAR}^f_4]$ and the low coordinate aminoboryl complex $[\text{Rh}(\text{P}^i\text{Pr}_3)_2(\text{H})\text{-}(\text{BPhNMe}_2)][\text{BAR}^f_4]$. These results suggest that precatalysts which η^6 -bind arenes strongly should be avoided for the dehydrocoupling of amine–boranes bearing aryl substituents.

Received 15th January 2016,
Accepted 23rd February 2016

DOI: 10.1039/c6dt00197a

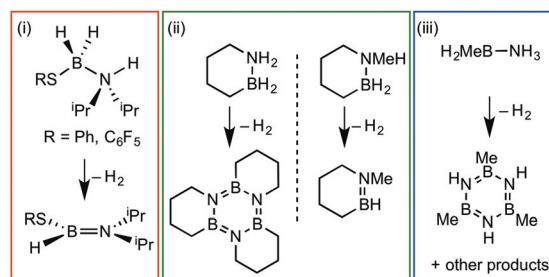
www.rsc.org/dalton

Introduction

Amine–boranes, defined by the simplest example $\text{H}_3\text{B}\cdot\text{NH}_3$, have been the subject of significant interest and research effort in the past decade with regard to their potential as molecular hydrogen storage materials (*i.e.* dehydrogenation)¹ and as precursors to polyaminoboranes (*i.e.* dehydrocoupling).² Much of this research has focussed on developing homo- and heterogeneous catalytic methodologies for dehydrogenation/dehydrocoupling that allow for control of kinetics and final product distributions.³ *N*-Alkyl substituted amine–boranes, particularly those bearing methyl groups⁴ (although aryl substituents are also known⁵) have received the bulk of attention because of their thermal stability (*N*-alkyl especially as *N*-aryl undergo spontaneous dehydrocoupling^{5b}) relative ease of synthesis, high weight% H, and as precursors to polyaminoboranes.⁴ The coordination chemistry, and subsequent reactivity, of such species is also well developed, often operating through 3 centre–2 electron (3c–2e) sigma $\text{M}\cdots\text{H}\text{-B}$ interactions.^{3,4,6} Developments in *B*-substituted analogues have, surprisingly,

lagged behind; perhaps due to their more challenging synthesis,⁷ and potential instability due to weaker B–N bonds.^{7b,8}

The reactivity and coordination chemistry of *B*-alkyl (or heteroalkyl) substituted amine–boranes, particularly with respect to dehydrocoupling, has only recently attracted significant attention. Manners and co-workers reported the synthesis of *B*-substituted amine–boranes containing relatively exotic substituents [*e.g.* C_6F_5 or SR, Scheme 1(i)]⁹ that undergo dehydrogenation to form the corresponding aminoboranes. Liu and co-workers have developed a range of cyclic amine–boranes [selected examples shown in Scheme 1(ii)],¹⁰ that can be dehydrocoupled by transition metal catalysts to form discrete, well-characterised products.¹¹ In some cases intermedi-

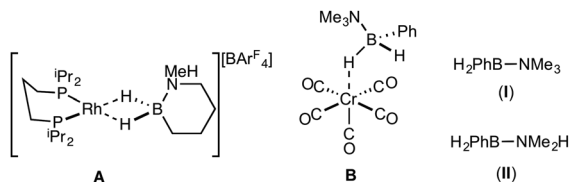


Scheme 1 Selected examples of *B*-substituted amine–boranes and the products of dehydrogenation.

Department of Chemistry, University of Oxford, 12 Mansfield Road, Oxford, OX1 3TA, UK. E-mail: andrew.weller@chem.ox.ac.uk

† Electronic supplementary information (ESI) available. CCDC 1445275–1445282. For ESI and crystallographic data in CIF or other electronic format see DOI: 10.1039/c6dt00197a



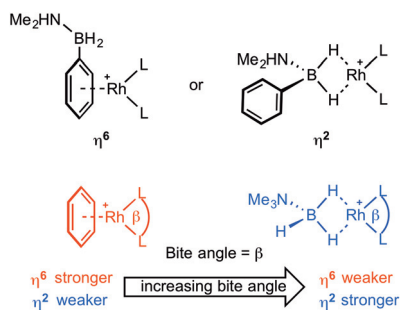


Scheme 2 Coordination complexes of *B*-substituted amine-boranes, and *B*-aryl precursors used in this study. Ar^F = 3,5-(CF₃)₂C₆H₃.

ate sigma-complexes can be isolated, *e.g.* A Scheme 2.^{11f} Liu and Manners have independently described the dehydrogenation of the *B*-methyl amine-boranes MeH₂B-NMe_xH_{3-x} [*x* = 0, 1, 2; Scheme 1(iii)] by catalytic and non-catalytic (thermal) routes.⁷

Reports of *B*-aryl amine-boranes are scarce. H₂PhB-NMe₃ (**I**)¹² has been shown to form sigma-complexes with suitable group 6 and 7 metal fragments (*e.g.* **B**, Scheme 2).¹³ H₂PhB-NMe₂H (**II**) is known¹⁴ but its coordination chemistry or dehydrocoupling has not been reported. The *B*-phenyl amine-borane H₂PhB-NH₃ can be dehydrocoupled using [Pd(NCMe)₄][BF₄]₂ to form a material tentatively identified as [PhBNH_x]_n, but insolubility prevented further characterisation.¹⁵

We report here a detailed study into the coordination chemistry of *B*-aryl substituted amine-boranes (**I**) and (**II**) with {Rh(L₂)}⁺ fragments (L₂ = (PR₃)₂ or chelating diphosphine) in which the steric and electronic (bite angle, β¹⁶) demands of the phosphine ligands are varied. Unlike *B*-alkyl (or *N*-alkyl) substituted amine-boranes, *B*-aryl analogues offer two potential binding motifs: either through the aryl (*e.g.* η⁶) or 3c-2e Rh...H-B interactions (*e.g.* η²), Scheme 3. The relative strength of amine-borane sigma binding with increasing bite angle has been commented upon before in [Rh(L₂)(η²-H₃B-NMe₃)] [BAR^F]₄ complexes, with larger L-Rh-L bite angles favouring tighter Rh...H₂B interactions (as measured by NMR spectroscopy).¹⁷ Conversely, larger bite angles in the simple arene complexes [Rh(L₂)(η⁶-C₆H₅F)] [BAR^F]₄ result in weaker Rh...arene interactions, as measured by collision-induced dissociation in Electrospray Mass Spectrometry (ESI-MS) and solution equilibrium measurements.¹⁸ These trends presumably reflect the



Scheme 3 Potential coordination modes of *B*-aryl amine-boranes with {Rh(L₂)}⁺ fragments, and previous observations regarding bite angle and strength of binding of a generic arene and amine-borane fragments.

optimisation of bonding between the d⁸-Rh(i)-{ML₂} fragment and either the B-H sigma donating orbitals¹³ or the π-arene orbitals,¹⁹ as modified by the L-Rh-L angle.²⁰ This can be interpreted by the energy of the C_{2v}-{ML₂}⁺ LUMO that is of π-symmetry (b₁) becoming lower in energy with increasing bite angle,^{17a,21} thus finding a worse match with the arene HOMO and a better one with the relatively low lying B-H σ-orbitals. In this contribution we demonstrate empirically that with *B*-aryl amine-boranes the L-Rh-L bite-angle dictates which mode of binding is observed (*i.e.* η⁶ or η²), present equilibrium thermochemical data on the relative binding strengths of each motif when the two binding modes are finely balanced, and show that dehydrocoupling of H₂PhB-NMe₂H forms an unusual example of a *B*-substituted acyclic aminoborane which undergoes subsequent B-H activation to form a *B*-substituted amino-boryl complex.

Results and discussion

Synthesis of precursors

H₂PhB-NMe₃ (**I**)¹² and H₂PhB-NMe₂H (**II**)¹⁴ have been reported, and their original syntheses comes from the reaction of di-boranes (PhBH₂)₂ with NMe₃ or NMe₂H respectively. An alternative, expedient, synthesis of (**I**) and (**II**) is based on the methods of Hawthorne,²² Shimoi,¹³ and Liu.^{7a} Li[PhBH₃], prepared by reaction of phenylboronic acid with lithium aluminium hydride in diethyl ether,²³ was combined with the appropriate ammonium salt, [NMe₃H]Cl or [NMe₂H₂]Cl, to give H₂PhB-NMe₃ (**I**) and H₂PhB-NMe₂H (**II**) respectively, which were isolated as white solids in good yield. NMR spectroscopic data for (**I**) in CD₂Cl₂ are consistent those previously described¹³ [*e.g.* BH₂: δ(¹H) 2.37; δ(¹¹B) -0.8, t, J(BH) 97 Hz], while as far as we are aware NMR data for (**II**) have not been previously reported; BH₂: δ(¹H) 2.34; δ(¹¹B) -4.7, t, J(BH) 95 Hz. In contrast to *N*-aryl amine boranes, such as H₃B-NPhH₂,^{5b} compounds (**I**) and (**II**) were found to be stable towards thermal dehydrocoupling or B-N bond cleavage, remaining unchanged on heating (C₆H₅F, 80 °C, 12 h).

Coordination chemistry of H₂PhB-NMe₃

Reaction of a stoichiometric amount of (**I**) with [Rh(L₂)(η⁶-C₆H₅F)] [BAR^F]₄ [L₂ = (PⁱPr₃)₂,²⁴ (PⁱBu₃)₂,²⁵ ⁱPr₂P(CH₂)₃PⁱPr₂,^{18b} Ph₂P(CH₂)₃PPh₂ and Ph₂P(CH₂)₅PPh₂^{17b}] in 1,2-difluorobenzene solvent resulted in displacement of the fluorobenzene ligand and formation of new complexes in solution as determined by NMR spectroscopy. These fragments were chosen to probe changes in phosphine bite-angle, while keeping the electronic contribution from the phosphine substituent as constant as possible. For example PⁱBu₃ and PⁱPr₃ have different cone angles of 143° & 160° respectively but similar electronic properties;²⁶ L-Rh-L bite angles can be varied in Ph₂P(CH₂)_nPPh₂ (*n* = 3 or 5); and mono-dentate *versus* chelating coordination modes can be probed with PⁱPr₃ and ⁱPr₂P(CH₂)₃PⁱPr₂. These fragments have also been used to form well-defined sigma amine-borane complexes with, for



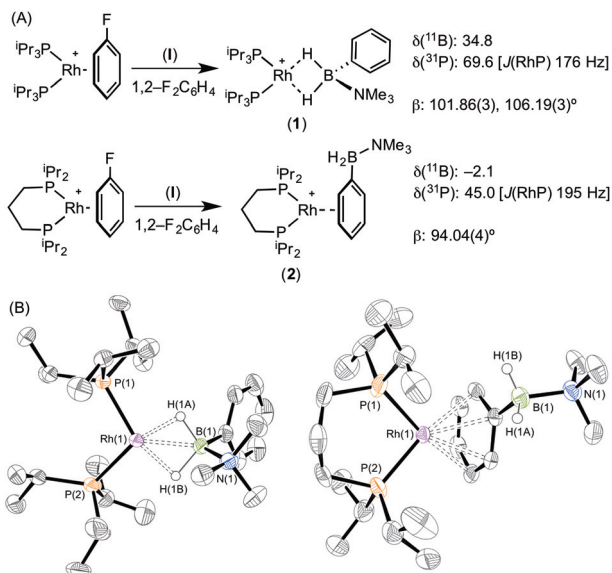
example, $\text{H}_3\text{B}\cdot\text{NR}_3$ type ligands,^{11f,17,27} whose structures and solution NMR spectroscopic markers are well-established.

The reaction of $[\text{Rh}(\text{P}^i\text{Pr}_3)_2(\eta^6\text{-C}_6\text{H}_5\text{F})][\text{BAR}^{\text{F}}_4]$ with **(I)** resulted in the immediate formation of a deep purple solution. Recrystallisation by addition of pentane gave blue crystalline material in 69% isolated yield, identified by NMR spectroscopy and single crystal X-ray diffraction as $[\text{Rh}(\text{P}^i\text{Pr}_3)_2(\eta^2\text{-H}_2\text{PhB}\cdot\text{NMe}_3)][\text{BAR}^{\text{F}}_4]$ (**1**) in which the amine–borane binds through two $\text{Rh}\cdots\text{H}\text{--B}$ 3c–2e interactions (Scheme 4). In the $^{11}\text{B}\{^1\text{H}\}$ NMR spectrum a single broad peak is observed at δ 34.8, with a characteristic downfield shift (35.6 ppm) of the borane resonance compared to free ligand (δ –0.8) that signals η^2 $\text{Rh}\cdots\text{H}\text{--B}$ binding.^{27,28} In the ^1H NMR spectrum the BH_2 resonance is observed at δ –6.36 (2 H relative integral), an upfield shift of 8.73 ppm compared to free ligand. The aryl protons [δ 7.37, 3H; δ 7.25, 2H] are not significantly shifted from free ligand.¹³ In the $^{31}\text{P}\{^1\text{H}\}$ NMR spectrum a doublet is observed at δ 69.6 [$J(\text{RhP}) = 176$ Hz], shifted 14.1 ppm downfield from the starting material.²⁴ In the solid state the complex crystallises with two cations (and two anions) in the asymmetric unit. An overlay of the independent cations (ESI) did not reveal any significant difference in amine–borane geometry but the P^iPr_3 ligands vary slightly in position and conformation [e.g. $\text{P}(1)\text{--Rh}(1)\text{--P}(2)$ 106.19(3) Å, $\text{P}(3)\text{--Rh}(2)\text{--P}(4)$ 101.86(3)°] which we

attribute to crystal packing effects due to a rather flat potential energy surface as only one set of resonances could be observed in the ^1H , ^{11}B and $^{31}\text{P}\{^1\text{H}\}$ NMR spectra. This observation of different ligand conformation/bite angles of two independent molecules in the asymmetric unit has been noted in amine–borane complexes of $\text{H}_3\text{B}\cdot\text{NMe}_2\text{BH}_2\cdot\text{NMe}_2\text{H}$ and $[\text{Me}_2\text{NBH}_2]_2$ with the $\{\text{Rh}(\text{P}^i\text{Bu}_3)_2\}^+$ fragment.²⁷ In the solid-state short $\text{Rh}\cdots\text{B}$ distances [2.150(3) and 2.159(3) Å] are consistent with an η^2 -binding mode, by comparison to previously reported structures,^{17b,27,29} including sigma amine–borane complexes of closely related $^t\text{BuCH}_2\text{CH}_2\text{BH}_2\cdot\text{NMe}_3$.³⁰ This distance in the structurally similar $[\text{Rh}(\text{P}^i\text{Pr}_3)_2(\eta^2\text{-H}_3\text{B}\cdot\text{NMe}_3)][\text{BAR}^{\text{F}}_4]$ is slightly shorter [2.1376(3) Å],^{17a} perhaps as a result of the extra steric demand caused by *B*-substitution in **1**. High quality X-ray diffraction data allowed the hydrogen atoms of the BH_2 unit to be located in the difference map and refined freely, confirming the η^2 -coordination mode.

Forcing the P–Rh–P bite angle to be significantly smaller, while keeping the electronic contribution of the P-substituents the same, is achieved by use of the chelating phosphine complex $[\text{Rh}(\text{P}^i\text{Pr}_2\text{P}(\text{CH}_2)_3\text{P}^i\text{Pr}_2)(\eta^6\text{-C}_6\text{H}_5\text{F})][\text{BAR}^{\text{F}}_4]$. Reaction of this with a stoichiometric amount of amine–borane (**I**) resulted in the formation of an orange solution, rather than the purple one observed for **1**. X-ray diffraction quality crystals were obtained from a 1,2-difluorobenzene/pentane recrystallisation, from which a single crystal X-ray diffraction study demonstrated η^6 -binding of the arene, rather than $\text{Rh}\cdots\text{H}\text{--B}$ bonding: $[\text{Rh}(\text{P}^i\text{Pr}_2\text{P}(\text{CH}_2)_3\text{P}^i\text{Pr}_2)(\eta^6\text{-PhH}_2\text{B}\cdot\text{NMe}_3)][\text{BAR}^{\text{F}}_4]$ (**2**) (Scheme 4B). The P–Rh–P bite angle [94.04(4)°] is significantly smaller than in η^2 -bound complex **1** [e.g. 101.86(3)°]. Consistent with this different binding mode, that does not involve the borane fragment, in the $^{11}\text{B}\{^1\text{H}\}$ NMR spectrum a single resonance is observed at δ –2.1 that is now only slightly shifted from free amine–borane (δ –0.8). In the $^{31}\text{P}\{^1\text{H}\}$ NMR spectrum a single species is observed [δ 45.0; $J(\text{RhP}) = 195$ Hz] a chemical shift that is barely changed when compared with $[\text{Rh}(\text{P}^i\text{Pr}_2\text{P}(\text{CH}_2)_3\text{P}^i\text{Pr}_2)(\eta^6\text{-C}_6\text{H}_5\text{F})][\text{BAR}^{\text{F}}_4]$.^{18b} No resonance was observed in the high-field region of the ^1H NMR spectrum that would signal $\text{Rh}\cdots\text{H}_2\text{B}$ interactions, but peaks at δ 6.93 [relative integral 1 H] and δ 6.31 [4 H, a 2 + 2 coincidence] demonstrate η^6 -binding through the phenyl moiety of **(I)**.³¹ Thus a change in the bite angle from 101.83(3)° in **(1)** to 94.04(4)° in **(2)** is also reflected in a change in the coordination mode from η^2 to η^6 .

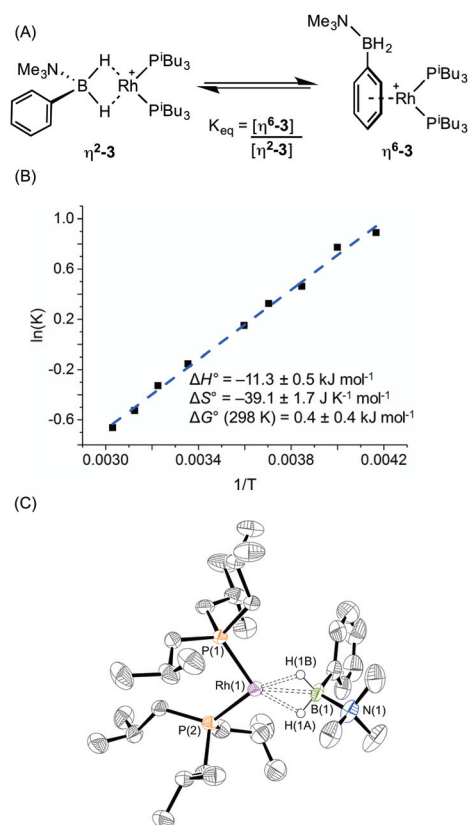
This preference comes into fine balance when the monodentate phosphine P^iBu_3 is used, that has a cone angle of 143° and thus might be expected to have a smaller P–Rh–P bite angle than **(1)**.^{17a} Reaction of **(I)** with the precursor complex $[\text{Rh}(\text{P}^i\text{Bu}_3)_2(\eta^6\text{-C}_6\text{H}_5\text{F})][\text{BAR}^{\text{F}}_4]$ again led to formation of a purple solution. However, more complicated NMR data were observed than for either **(1)** or **(2)** which suggested the presence of two species in solution. In the $^{11}\text{B}\{^1\text{H}\}$ NMR spectrum (CD_2Cl_2) two peaks are observed at δ 29.5 and –2.1 in a ratio of 10 : 11 respectively. The peak observed at δ 29.5 suggested the formation of a sigma complex with a η^2 - $\text{Rh}\cdots\text{H}_2\text{B}$ interaction, being shifted 30.3 ppm downfield compared to **I**, *cf.* complex **(1)**. The higher field signal at δ –2.1 is only shifted 1.3 ppm



Scheme 4 (A) Synthesis, selected NMR spectroscopic data and (B) molecular structures of $[\text{Rh}(\text{P}^i\text{Pr}_3)_2(\eta^2\text{-H}_2\text{PhB}\cdot\text{NMe}_3)][\text{BAR}^{\text{F}}_4]$ (**1**) and $[\text{Rh}(\text{P}^i\text{Pr}_2\text{P}(\text{CH}_2)_3\text{P}^i\text{Pr}_2)(\eta^6\text{-H}_2\text{PhB}\cdot\text{NMe}_3)][\text{BAR}^{\text{F}}_4]$ (**2**). $[\text{BAR}^{\text{F}}_4]^-$ anions and selected H atoms are omitted for clarity. Ellipsoids shown at 50% probability level. Selected bond lengths (Å) and angles (°) (**1**) [values are also given for the second cation in the asymmetric unit which is not shown in the figure]: $\text{Rh}(1)\text{--P}(1)$ 2.2581(6), $\text{Rh}(1)\text{--P}(2)$ 2.2748(7), $\text{Rh}(1)\text{--B}(1)$ 2.150(3), $\text{B}(1)\text{--N}(1)$ 1.623(4), $\text{Rh}(2)\text{--P}(3)$ 2.2628(7), $\text{Rh}(2)\text{--P}(4)$ 2.2655(7), $\text{Rh}(2)\text{--B}(2)$ 2.159(3), $\text{B}(2)\text{--N}(2)$ 1.629(4), $\text{P}(1)\text{--Rh}(1)\text{--P}(2)$ 106.19(3), $\text{P}(3)\text{--Rh}(2)\text{--P}(4)$ 101.86(3). (**2**) [Only major component of disorder shown]. Ellipsoids shown at 50% probability level. Selected bond lengths (Å) and angles (°): $\text{Rh}(1)\text{--P}(1)$ 2.2340(9), $\text{Rh}(1)\text{--P}(2)$ 2.2403(8), $\text{Rh}(1)\text{--Ph}$ centroid 1.848, $\text{B}(1)\text{--N}(1)$ 1.635(4), $\text{P}(1)\text{--Rh}(1)\text{--P}(2)$ 94.04(4).



upfield compared with free ligand suggesting an alternative coordination mode for the amine–borane, more like (2). In the $^{31}\text{P}\{^1\text{H}\}$ NMR spectrum two resonances are observed in the same ratio as measured in the ^{11}B NMR spectrum, one at δ 34.1 [d, $J(\text{RhP}) = 177$ Hz] with a similar downfield shift and coupling constant to (1), consistent with sigma complex formulation; while a signal at δ 25.2 [d, $J(\text{RhP}) = 202$ Hz] suggests a binding mode as for (2). These data indicate both $\eta^2\text{-Rh}\cdots\text{H}_2\text{B}$ and $\eta^6\text{-aryl}$ bound complexes are present in solution. The ^1H NMR spectrum is consistent with this description. In the high field region a broad resonance is observed at δ -5.06 ($\text{Rh}\cdots\text{H}_2\text{B}$) which integrates to 1.1 H relative to the $[\text{BAR}^{\text{F}}_4]^-$ signals, and 2 singlets are observed at δ 2.76 and 2.50 corresponding to NMe_3 protons in the different coordination modes of the amine–borane. In addition, resonances can be observed upfield of the aryl region indicative of $\eta^6\text{-aryl}$ coordination. These two complexes are formulated as $[\text{Rh}(\text{P}^i\text{Bu}_3)_2(\eta^2\text{-H}_2\text{PhB-NMe}_3)][\text{BAR}^{\text{F}}_4]$ ($\eta^2\text{-3}$), and $[\text{Rh}(\text{P}^i\text{Bu}_3)_2(\eta^6\text{-PhH}_2\text{B-NMe}_3)][\text{BAR}^{\text{F}}_4]$ ($\eta^6\text{-3}$), Scheme 5A.



Scheme 5 (A) Equilibrium between $\eta^2\text{-3}$ and $\eta^6\text{-3}$, (B) Van't Hoff plot and (C) molecular structure of $[\text{Rh}(\text{P}^i\text{Bu}_3)_2(\eta^2\text{-H}_2\text{PhB-NMe}_3)][\text{BAR}^{\text{F}}_4]$ ($\eta^2\text{-3}$). The second cation in asymmetric unit, $[\text{BAR}^{\text{F}}_4]^-$ anions and selected H atoms are omitted for clarity. Only major component of disorder shown. Ellipsoids shown at 50% probability level. Selected bond lengths (Å) and angles (°) (values are also given for the second cation in the asymmetric unit which is not shown in the figure): Rh(1)–P(1) 2.2254(14), Rh(1)–P(2) 2.2436(14), Rh(1)–B(1) 2.153(6), B(1)–N(1) 1.605(8), Rh(2)–P(3) 2.2353(14), Rh(2)–P(4) 2.2289(14), Rh(2)–B(2) 2.172(6), B(2)–N(2) 1.617(9), P(1)–Rh(1)–P(2) 98.84(5), P(3)–Rh(2)–P(4) 95.14(5).

A variable temperature NMR spectroscopy study was carried out to determine if exchange between these isomers was occurring in solution. At 298 K in 1,2-difluorobenzene, the concentrations of $\eta^2\text{-3}$ and $\eta^6\text{-3}$ were found to be approximately equal. Lowering the temperature to 240 K resulted in a relative increase in $\eta^6\text{-3}$ while at higher temperature (330 K) ($\eta^2\text{-3}$) was favoured, demonstrating the two isomers to be in dynamic equilibrium. The equilibrium constant at each temperature was calculated from integration of the $^{31}\text{P}\{^1\text{H}\}$ NMR spectra; and the resulting Van't Hoff plot (Scheme 5B) allowed for determination of the thermodynamic parameters for this exchange: $\Delta H^\circ = -11.3 \pm 0.5 \text{ kJ mol}^{-1}$; $\Delta S^\circ = -39.1 \pm 1.7 \text{ J K}^{-1} \text{ mol}^{-1}$; $\Delta G(298 \text{ K}) = 0.4 \pm 0.4 \text{ kJ mol}^{-1}$. Thus binding between the two modes is approximately thermoneutral. The negative enthalpy indicates $\eta^6\text{-binding}$ of the aryl group is stronger than the $\eta^2\text{-binding}$ through BH_2 but this is moderated by the associated negative entropy, which is likely to be the result of loss of free rotation of the phenyl group upon $\eta^6\text{-binding}$. The negative entropy also means that $\eta^2\text{ Rh}\cdots\text{H-B}$ binding will become increasingly favoured at higher temperature. A similar entropy change ($\Delta S^\circ = -16.3 \pm 3.3 \text{ J K}^{-1} \text{ mol}^{-1}$) upon loss of phenyl group free rotation was observed in the epimerisation of 2-phenyl-*c*-4,*c*-6-dimethyl-1,3-dioxane;³² while for the anion exchange equilibrium between $[\text{1-closo-CB}_{11}\text{H}_6\text{Br}_6]^-$ and $[\text{BAR}^{\text{F}}_4]^-$ $\eta^6\text{-binding}$ through an aryl group of $[\text{BAR}^{\text{F}}_4]^-$ was also shown to be enthalpically favoured but entropically disfavoured ($\Delta S^\circ = -87.6 \pm 0.8 \text{ J K}^{-1} \text{ mol}^{-1}$).³³

Layering a 1,2-difluorobenzene solution of this mixture with pentane at -30°C led to formation of purple crystals and an orange oil. Isolation of a crystal suitable for X-ray diffraction by mechanical separation allowed the solid-state structure of the purple material to be determined (Scheme 5C). As for complex (1), two cations are present in the asymmetric unit; an overlay of these independent structures (ESI) did not reveal significant differences in amine–borane binding and orientation, although some conformational differences and a difference in ligand bite angle was observed for the P^iBu_3 ligands. The structure shows a close interaction between the rhodium centre and the BH_2 moiety in $[\text{Rh}(\text{P}^i\text{Bu}_3)_2(\eta^2\text{-H}_2\text{PhB-NMe}_3)][\text{BAR}^{\text{F}}_4]$ ($\eta^2\text{-3}$) with $\text{Rh}\cdots\text{B}$ distances of 2.153(6) and 2.172(6) Å consistent with $\eta^2\text{-binding}$. Although the hydrogen atoms could not be located in the difference map and were placed in calculated positions, the metrical data are consistent with this description as well as the NMR data. The two P–Rh–P bite angles measured for each independent molecule, 95.14(5) and 98.84(5)°, are smaller than for (1), but larger than for (2), consistent with the equilibrium observed in solution. $[\text{Rh}(\text{P}^i\text{Bu}_3)_2(\eta^6\text{-C}_6\text{H}_5\text{F})][\text{BAR}^{\text{F}}_4]$, a model for $\eta^6\text{-binding}$ of (1), has a P–Rh–P angle of 94.14(4)°, placing the approximate tipping point between the two structural motifs as lying between 94 and 95°.

Bulk mechanical separation of the crystals from the oil for further analysis was not possible, but we propose the orange oil to be the $\eta^6\text{-phenyl}$ bound amine–borane complex $[\text{Rh}(\text{P}^i\text{Pr}_3)_2(\eta^6\text{-PhH}_2\text{B-NMe}_3)][\text{BAR}^{\text{F}}_4]$ ($\eta^6\text{-3}$). Dissolving the mixture of blue crystals and orange oil isolated gave a solution



that showed the same NMR spectra as a freshly prepared sample.

To extend this study into the effect of bite angle $[\text{Rh}(\text{Ph}_2\text{P}(\text{CH}_2)_5\text{PPh}_2)(\eta^6\text{-C}_6\text{H}_5\text{F})][\text{BAR}^{\text{F}}_4]$ was used as a starting material, which has a flexible chelating phosphine with a 5-carbon backbone. This ligand has been shown to be able to access to a wide range of bite angles, and values of $93.98(4)$ to $117.3(1)^\circ$ have been determined crystallographically.^{16b,34} Reaction of a stoichiometric amount of this starting material with **(I)** resulted in an orange solution with NMR data characteristic of an η^6 -aryl bound. Crystallisation from layering a dichloromethane solution with pentane allowed a single crystal X-ray diffraction study to be carried out and confirmed the η^6 -coordination mode in $[\text{Rh}(\text{Ph}_2\text{P}(\text{CH}_2)_5\text{PPh}_2)(\eta^6\text{-PhH}_2\text{B-NMe}_3)][\text{BAR}^{\text{F}}_4]$ (**4**) (Fig. 1). The phosphine ligand bite angle was found to be only $92.21(4)^\circ$, the smallest observed crystallographically for this ligand but consistent with the observed binding mode. By contrast the corresponding $\text{H}_3\text{B-NMe}_3$ complex is η^2 -bound, $[\text{Rh}(\text{Ph}_2\text{P}(\text{CH}_2)_5\text{PPh}_2)(\eta^2\text{-H}_3\text{B-NMe}_3)][\text{BAR}^{\text{F}}_4]$, and shows a P-Rh-P bite angle of $98.18(3)^\circ$. This shows that the observed bite angle for a flexible ligand such as $\text{Ph}_2\text{P}(\text{CH}_2)_5\text{PPh}_2$ is very dependent on the ancillary ligands. The analogous complex formed with the smaller bite angle aryl diphosphine, $[\text{Rh}(\text{Ph}_2\text{P}(\text{CH}_2)_3\text{PPh}_2)(\eta^6\text{-PhH}_2\text{B-NMe}_3)][\text{BAR}^{\text{F}}_4]$ (**5**), $87.955(15)^\circ$, ESI also shows a η^6 -coordination mode. The data for the ligation of **(I)** is summarised in Fig. 2; in which a plot of Rh...B distance against bite angle shows that larger bite angles give η^2 -complexes, smaller bite angles result in η^6 -complexes, with a crossover point at approximately 95° . The Rh...B distance in the η^2 -binding mode appears to be rather insensitive to bite angle.

Catalytic dehydrogenation of $\text{H}_2\text{PhB-NMe}_2\text{H}$ (**II**)

$\{\text{Rh}(\text{P}_2)\}^+$ fragments have been shown to catalyse the dehydrocoupling of secondary and primary amine-boranes;^{17,27} and the ligand bite angle has been shown to affect the rate of de-

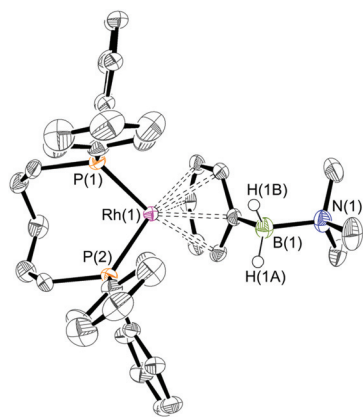


Fig. 1 X-ray molecular structure of $[\text{Rh}(\text{Ph}_2\text{P}(\text{CH}_2)_5\text{PPh}_2)(\eta^6\text{-PhH}_2\text{B-NMe}_3)][\text{BAR}^{\text{F}}_4]$ (**4**). $[\text{BAR}^{\text{F}}_4]^-$ anion and selected H atoms omitted for clarity. Ellipsoids shown at 50% probability level. Selected bond lengths (Å) and angles ($^\circ$): Rh(1)–P(1) 2.2416(8), Rh(1)–P(2) 2.2469(7), Rh(1)–Ph centroid 1.860, B(1)–N(1) 1.638(3); P(1)–Rh(1)–P(2) $92.21(4)$.

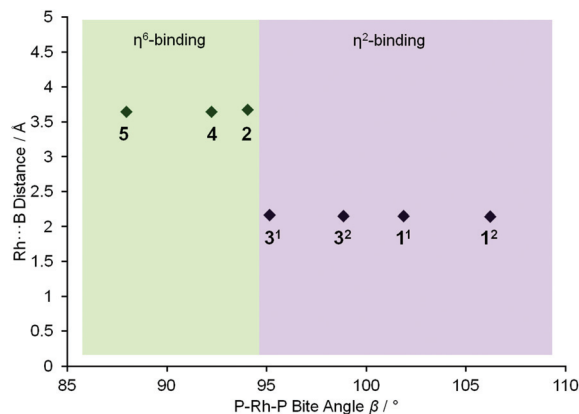
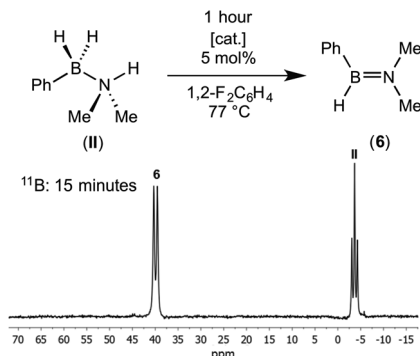


Fig. 2 Plot of Rh...B distance against bite angle β showing different binding modes for complexes **1**, **2**, **3**, **4** and **5**. The values for independent cations in the asymmetric units of **1** and **3** are given separately.

hydrocoupling of $\text{H}_3\text{B-NMe}_2\text{H}$ in particular.¹⁷ Although empirically it is found that the smaller bite angles promoted in larger turnover frequencies, the precise factors behind these differences are not yet fully delineated and likely involve a combination of relative accessibility of Rh(I)/Rh(III) oxidation states/ease of H_2 loss/relative barriers to BH and NH activation all as modified by the bite angle.^{3,35} We therefore sought to probe the effect of the ligands on the dehydrocoupling of secondary amine-borane (**II**) by comparing two electronically similar precatalysts but with very different P-Rh-P angles: $[\text{Rh}(\text{P}^i\text{Pr}_2)_2(\eta^6\text{-C}_6\text{H}_5\text{F})][\text{BAR}^{\text{F}}_4]$ and $[\text{Rh}(\text{P}^i\text{Pr}_2\text{P}(\text{CH}_2)_3\text{P}^i\text{Pr}_2)(\eta^6\text{-C}_6\text{H}_5\text{F})][\text{BAR}^{\text{F}}_4]$ which form η^2 and η^6 -complexes with **(I)**, *i.e.* (**1**) and (**2**) respectively.

Reaction of 5 mol% of these two precatalysts with **(II)** in 1,2-difluorobenzene (25°C , closed system) resulted in very slow³ consumption of **(II)** in both cases: less than 15% conversion in 5 hours (TOF less than 0.6 h^{-1}). Although slow, dehydrogenation is also not fast with other amine-boranes using these systems.^{11f,17a} The major ^{11}B -containing product displayed a single resonance at δ 39.4 which split into a doublet [$J(\text{BH}) = 123\text{ Hz}$] in the ^{11}B NMR spectrum. This was assigned as aminoborane $\text{HPhB}=\text{NMe}_2$ (**6**) from its characteristic ^{11}B NMR chemical shift and the presence of a single B-H bond (Scheme 6). For example aminoboranes bearing two alkyl groups at nitrogen show similar ^{11}B NMR chemical shift values (*e.g.* $\text{H}_2\text{B}=\text{NMe}_2$, δ 37.5; $\text{H}_2\text{B}=\text{NEt}_2$, δ 36.6; $\text{H}_2\text{B}=\text{N}^i\text{Pr}_2$, δ 35.1);³⁶ while the recently reported *B*-substituted $\text{HMeB}=\text{NMe}_2$, displays a doublet at δ 41.2 [$J(\text{BH}) = 123\text{ Hz}$] in the ^{11}B NMR spectrum,^{7b} and *cyclo*- $\text{HB}=\text{NMeC}_4\text{H}_8$ is observed at δ 40.8 [$J(\text{BH}) = 125\text{ Hz}$].^{11f} Heating to 77°C in a sealed NMR tube resulted in the complete consumption of **(II)** in less than 1 hour for both catalysts. The product (>95% by ^{11}B NMR spectroscopy) of dehydrocoupling was again found to be free aminoborane $\text{HPhB}=\text{NMe}_2$ from the *in situ* NMR spectrum. Unfortunately, due to its apparent instability and similar volatility to the 1,2-difluorobenzene solvent, separation and isolation of pure (**6**) was not possible due to decomposition upon vacuum distillation. Nevertheless NMR data are unambiguous,





Scheme 6 Catalytic dehydrogenation of amine-borane (**II**) to form aminoborane (**6**) at 77 °C [cat.] = $[\text{Rh}(\text{P}^i\text{Pr}_2)_2(\eta^6\text{-C}_6\text{H}_5\text{F})][\text{BAR}^{\text{F}}_4]$ or $[\text{Rh}(\text{P}^i\text{Pr}_2\text{P}(\text{CH}_2)_3\text{P}^i\text{Pr}_2)(\eta^6\text{-C}_6\text{H}_5\text{F})][\text{BAR}^{\text{F}}_4]$. Inset shows ^{11}B NMR spectrum after 15 minutes, [cat.] = $[\text{Rh}(\text{P}^i\text{Pr}_2\text{P}(\text{CH}_2)_3\text{P}^i\text{Pr}_2)(\eta^6\text{-C}_6\text{H}_5\text{F})][\text{BAR}^{\text{F}}_4]$.

and as we show *in situ* generated (**6**) can also be used for onward reactivity. The formation of (**6**) is in contrast with the metal catalysed dehydrocoupling of $\text{H}_2\text{MeB-NMe}_2\text{H}$ which forms cyclic *B*-dimethyl-*N*-tetramethyldiborazane,^{7b} $[\text{Me}_2\text{NBHMe}]_2$, as well as the aminoborane, $\text{HMeB}=\text{NMe}_2$. The *B*-phenyl group in (**6**) inhibits any appreciable dimerisation to the corresponding diborazane.

$[\text{Rh}(\text{Ph}_2\text{P}(\text{CH}_2)_3\text{PPh}_2)(\eta^6\text{-C}_6\text{H}_5\text{F})][\text{BAR}^{\text{F}}_4]$ has been shown to be an excellent catalyst for dehydrocoupling of $\text{H}_3\text{B-NMe}_2\text{H}$ (0.2 mol%, open system, TOF $\sim 1250 \text{ h}^{-1}$).^{17b} However this was also a slow catalyst for dehydrocoupling of (**II**) at room temperature, with full conversion to (**6**) only observed after 23 hours at 5 mol% catalyst loading (25 °C, TOF $\sim 1 \text{ h}^{-1}$). In order to probe the causes of the slow dehydrogenation of (**II**) with this catalyst, stoichiometric studies were performed.

Stoichiometric reactivity of $\text{H}_2\text{PhB-NMe}_2\text{H}$ (**II**)

The presence of the phenyl group which provides a competitive (η^6) site for amine-borane binding at the metal centre is a possible cause of the slow dehydrogenation of (**II**), as B-H activation at the metal centre requires the formation of a precursor sigma complex.^{2b,3} Preferential η^6 -coordination through the aryl ring makes this less likely.

Addition of a slight excess of (**II**) (1.2 equiv.) to $[\text{Rh}(\text{P}^i\text{Pr}_2\text{P}(\text{CH}_2)_3\text{P}^i\text{Pr}_2)(\eta^6\text{-C}_6\text{H}_5\text{F})][\text{BAR}^{\text{F}}_4]$ results in the formation of an η^6 -bound complex $[\text{Rh}(\text{P}^i\text{Pr}_2\text{P}(\text{CH}_2)_3\text{P}^i\text{Pr}_2)(\eta^6\text{-PhH}_2\text{B-NMe}_2\text{H})][\text{BAR}^{\text{F}}_4]$ (**7**) alongside a small amount of dehydrogenation product (**6**). Complex (**7**) was characterised by NMR spectroscopy and single crystal X-ray diffraction (Fig. 3). The solid-state structure reveals a ligand bite angle of $94.27(4)^\circ$ which is very similar to that in (**2**) [$94.04(4)^\circ$] which also displayed an η^6 -coordination mode. In addition to the expected resonances in the NMR spectra an N-H resonance is observed in the ^1H NMR spectrum at $\delta 3.55$. A similar complex is formed on reaction of $[\text{Rh}(\text{Ph}_2\text{P}(\text{CH}_2)_3\text{PPh}_2)(\eta^6\text{-C}_6\text{H}_5\text{F})][\text{BAR}^{\text{F}}_4]$ with (**II**), as characterised by NMR spectroscopy: $[\text{Rh}(\text{Ph}_2\text{P}(\text{CH}_2)_3\text{PPh}_2)(\eta^6\text{-PhH}_2\text{B-NMe}_2\text{H})][\text{BAR}^{\text{F}}_4]$ (**8**). When three equivalents of (**II**) were combined with $[\text{Rh}(\text{P}^i\text{Pr}_2\text{P}(\text{CH}_2)_3\text{P}^i\text{Pr}_2)(\eta^6\text{-C}_6\text{H}_5\text{F})][\text{BAR}^{\text{F}}_4]$

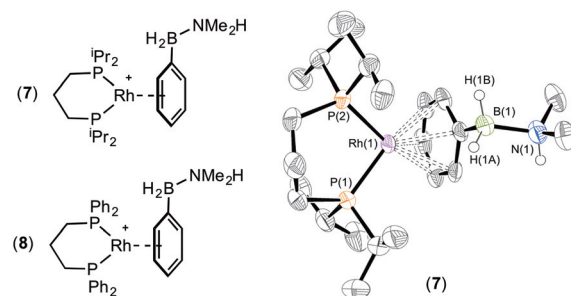


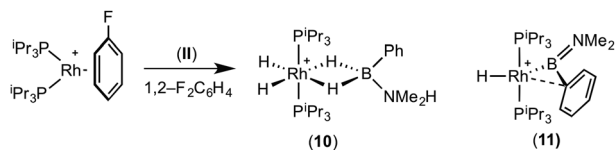
Fig. 3 X-ray molecular structure of (**7**). $[\text{BAR}^{\text{F}}_4]^-$ anion and selected H atoms omitted for clarity. Ellipsoids shown at 50% probability level. Selected bond lengths (Å) and angles ($^\circ$): Rh(1)-P(1) 2.2441(11), Rh(1)-P(2) 2.2422(10), Rh(1)-Ph centroid 1.851, B(1)-N(1) 1.618(6); P(1)-Rh(1)-P(2) 94.27(4).

slow dehydrocoupling (hours) to form aminoborane (**6**) occurs, with η^6 -bound (**7**) observed at the end of catalysis.

That η^6 -coordination of ligand (**II**) in (**7**) and (**8**) is preferred to η^2 -binding suggests that this competitive binding mode contributes to the slow dehydrogenation rate under catalytic conditions for these chelating systems. However, that dehydrogenation does occur catalytically, albeit slowly, indicates that if an inner sphere mechanism is operating, access to the η^2 -coordination mode through BH_2 is possible, but the equilibrium lies heavily in favour of η^6 -coordination. Complexes (**7**) and (**8**) do not dehydrogenate to any significant degree in the absence of exogenous amine-borane, and we, and others, have previously commented upon the role of B-H...H-N interactions in lowering barrier to dehydrocoupling.³⁷ Given the η^6 binding mode we cannot discount an outer-sphere mechanism in which π -coordination³⁸ of the metal activates the amine-borane to alternative dehydrogenation pathways. However, the N-H resonance does not change significantly on coordination [$\delta 3.55$ versus $\delta 3.52$] suggesting only a minimal perturbation to this bond.

By using a metal fragment which can adopt a large ligand bite angle, $\{\text{Rh}(\text{P}^i\text{Pr}_2)_2\}^+$, in which η^2 -coordination is favoured (*i.e.* complex **1**) this effect of competitive aryl binding can potentially be avoided. Upon mixing equal amounts of $[\text{Rh}(\text{P}^i\text{Pr}_2)_2(\eta^6\text{-C}_6\text{H}_5\text{F})][\text{BAR}^{\text{F}}_4]$ and (**II**) in 1,2- $\text{F}_2\text{C}_6\text{H}_4$ solvent a blue solution was immediately formed which rapidly decolourised (less than 5 min) to yield a very pale yellow solution. This blue colour likely results from the sigma-complex $[\text{Rh}(\text{P}^i\text{Pr}_2)_2(\eta^2\text{-H}_2\text{PhB-NMe}_2\text{H})][\text{BAR}^{\text{F}}_4]$, (**9**), although its short lifetime meant full characterisation was not possible. $^{31}\text{P}\{^1\text{H}\}$ NMR spectroscopy measured *in situ* after 2 minutes revealed three doublets [$\delta 69.3$, $J(\text{RhP}) = 174 \text{ Hz}$; $\delta 64.4$, $J(\text{RhP}) = 109 \text{ Hz}$; and $\delta 48.5$, $J(\text{RhP}) = 116 \text{ Hz}$] in an approximate ratio of 10:45:45 respectively. After 10 minutes the resonance at $\delta 69.3$ had disappeared leaving the remaining two in a 1:1 ratio. We propose the doublet at $\delta 69.3$ is therefore likely to result from (**9**). In the $^{11}\text{B}\{^1\text{H}\}$ NMR spectrum no signals for free (**II**) or (**6**) were observed. There was no further change after 24 hours. Recrystallisation at $-26 \text{ }^\circ\text{C}$ resulted in the formation





Scheme 7 Complexes (10) and (11). [BAR^F₄][−] anions not shown.

of two distinct crystalline products: colourless block- and pale yellow plate-type crystals that could be separated mechanically. Although relatively poor crystal quality compounded with significant disorder of the phosphine alkyl groups in both complexes prevented collection of high-quality data in single crystal X-ray diffraction experiments, the data were sufficient to identify the products as [Rh(PⁱPr₃)₂(H)₂(η²-H₂PhB-NMe₂H)][BAR^F₄][−] (10) and [Rh(PⁱPr₃)₂(H)(BPhNMe₂)] [BAR^F₄][−] (11), Scheme 7 and Fig. 4.

The solid-state structure of (10) contains two independent cations (and two anions) in the asymmetric unit with broadly similar metric parameters, but disorder is observed in the ⁱPr groups of the phosphine ligand. The N-H and B-H hydrogen atoms were placed in calculated positions, the Rh-H hydride ligands could not be reliably placed and so were omitted, although their presence was confirmed by NMR spectroscopy and ESI-MS of pure, isolated material, *vide infra*. The structure, and NMR data, of (10) are similar to the closely related complex [Rh(PⁱPr₃)₂(H)₂(η²-H₃B-NMe₃)] [BAR^F₄][−],^{17a} with the PⁱPr₃ ligands in *trans* orientation, *cis* Rh-H functionality and Rh-B distances of 2.274(9) and 2.333(8) Å respectively]. The

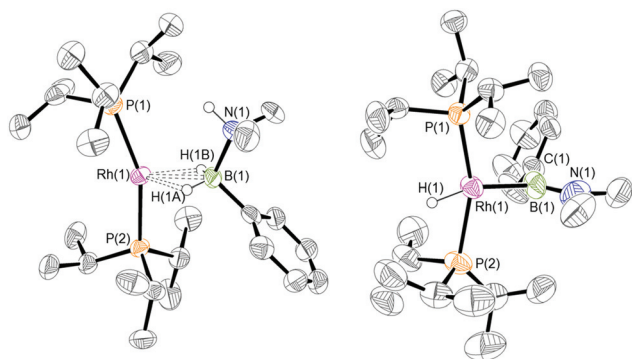


Fig. 4 X-ray molecular structures of [Rh(H)₂(PⁱPr₃)₂(η²-H₂PhB-NMe₂H)][BAR^F₄][−] (10), left, one independent cation from the asymmetric unit is shown; and [Rh(H)(PⁱPr₃)₂(BPhNMe₂)] [BAR^F₄][−] (11), right. [BAR^F₄][−] anions, minor components of disorder and selected H atoms omitted for clarity. Ellipsoids shown at 50% probability level. Selected bond lengths (Å) and angles (°). (10) [Values are also given for the second cation in the asymmetric unit which is not shown in the figure]: Rh(1)–P(1) 2.336(2), Rh(1)–P(2) 2.330(2), Rh(1)–B(1) 2.274(9), B(1)–N(1) 1.650(11), Rh(2)–P(3) 2.3227(19), Rh(2)–P(4) 2.327(2), Rh(2)–B(2) 2.333(8), B(2)–N(2) 1.608(11), P(1)–Rh(1)–P(2) 158.35(8), P(3)–Rh(2)–P(4) 155.75(8). (11): Rh(1)–P(1) 2.3292(18), Rh(1)–P(2) 2.350(2), Rh(1)–B(1) 1.929(9), B(1)–C(1) 1.536(14), B(1)–N(1) 1.411(14), P(1)–Rh(1)–P(2) 157.55(7), P(1)–Rh(1)–B(1) 100.2(3), P(2)–Rh(1)–B(1) 100.6(3), Rh(1)–B(1)–N(1) 138.0(8), Rh(1)–B(1)–C(1) 98.3(7), N(1)–B(1)–C(1) 123.7(8).

³¹P{¹H} NMR spectrum (CD₂Cl₂) of isolated (10) confirmed this species as one of the products observed in the mixture, δ 64.7 [d, *J*(RhP) = 108 Hz]. Presumably the amine–borane in (10) is undergoing a fluxional process that makes the phosphine ligands equivalent at room temperatures, similar to that observed in related complexes³⁹ in which an η² to η¹ change in coordination is accompanied by a rotation around the Rh...H–B bond. In the ¹H NMR spectrum a broad resonance at δ –2.08 is assigned to the Rh...H₂B interaction, and a sharper one at δ –19.05 (integral 2 H) assigned to Rh–H. The ¹¹B{¹H} NMR spectrum shows a signal at δ 8.0 assigned to the amine–borane. ESI-MS confirmed the formulation of the cation to be [Rh(PⁱPr₃)₂(H)₂(η²-H₂PhB-NMe₂H)]⁺ (*m/z* = 560.32 (found), 560.32 (calculated)). Complex (10) forms by sequential B–H/N–H activation at a Rh(I) centre, to form a Rh(III) dihydride, which then coordinates another equivalent of (II) to liberate free (6). Such activation processes are well established.^{3,27}

The second product isolated from the reaction mixture, [Rh(PⁱPr₃)₂(H)(BPhNMe₂)] [BAR^F₄][−] (11), is more unusual. The solid-state structure shows a complex in which the phosphine ligands are arranged in a *trans* orientation, and a molecule of aminoborane (6) has undergone overall oxidative addition of the B–H bond at the {Rh(PⁱPr₃)₂}⁺ fragment to form a terminal hydride (located in the final difference map) and a direct Rh–B bond, *i.e.* an amino–boryl species.

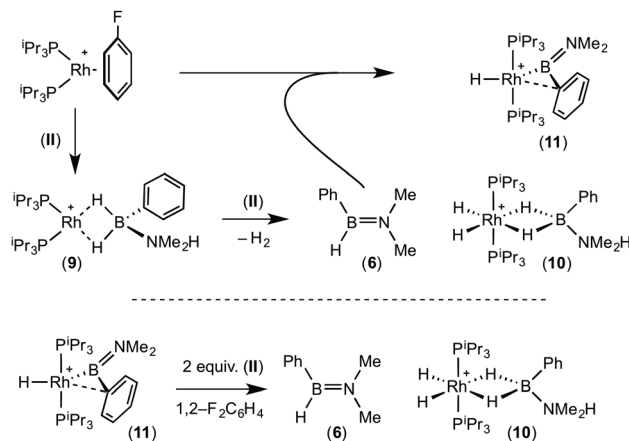
Group 9 amino–boryl species have been isolated previously, coming from B–H activation, *e.g.* [Rh(IMes)₂(H){B(H)=NMe₂}]⁺ [C, IMes = *N,N*-bis(2,4,6-trimethylphenyl)imidazol-2-ylidene]⁴⁰ or [Rh(κ³-^t-POP-Xantphos)(H)(B(H)=NⁱPr₂(NCMe))] [BAR^F₄][−].⁴¹ The Rh–B distance in (11) [1.929(9) Å] is, within error, the same as that found in (C) [1.960(9) Å]. A relatively short B–N bond [1.411(14) Å, cf (C) 1.390(15) Å] suggests aminoborane character is retained, and the B–C_{aryl} bond distance of 1.536(14) Å is consistent with a single bond. The angles around boron sum to 360°, demonstrating sp² character, although the Rh–B(1)–C(1) angle of 98.3(7)° is much smaller than might be expected for such hybridisation. Overall these metrics point to an amino–boryl species, rather than an alternative borylene structure.⁴² There appears to be a vacant site that sits *cis* to Rh–H and Rh–B. There are no close^{25,43} Rh...C interactions from the ⁱPr ligands that would point to an agostic interaction [shortest Rh...C 3.227 Å]. There is, however, a relatively short Rh...C distance to the *ipso*-phenyl carbon atom [2.634(8) Å] that, when combined with the compressed Rh–B–C angle, suggests a Rh...C(*ipso*) interaction. The next closest distance to the phenyl group is 3.042(9) Å (*ortho* carbon), longer than would be expected for a η²-arene type interaction. The geometry is reminiscent of the η²-benzyl complexes that interact *via* methylene and *ipso* carbon atoms.⁴⁴ Including the Rh...C(*ipso*) interaction complex (11) can be described as a 16-electron Rh(III) species, and (11) is also related to the 16-electron Rh(PⁱPr₃)₂(Bcat)(H)Cl that comes from oxidative addition of HBcat to a Rh(I) precursor (cat = catechol).⁴⁵ Interestingly, in the system when a chelating phosphine is used an η⁶-complex is isolated, Rh(ⁱPr₂PCH₂CH₂PⁱPr₂){(η⁶-cat)Bcat}, paralleling the observations described herein.



In the $^{31}\text{P}\{^1\text{H}\}$ NMR spectrum of (**11**) a doublet is observed [δ 48.8, $J(\text{RhP}) = 120$ Hz]. The chemical shift of δ 50.1 for the aminoborane observed in the $^{11}\text{B}\{^1\text{H}\}$ NMR spectrum places the complex as a boryl, rather than a borylene⁴² [cf. aminoboryl (**C**) δ 50.1]. The ^1H NMR spectrum displays the terminal Rh–H at δ –21.71 [doublet of triplets, $J(\text{RhH}) = 64$ Hz, $J(\text{PH}) = 12$ Hz], the unusually large Rh–H coupling constant^{31a} indicates a hydride bound to low coordinate Rh(III) centre; e.g. (**C**) $J(\text{RhH}) = 43$ Hz.^{40a} or $[\text{Rh}(\text{P}^t\text{Bu}_3)_2(\eta^6\text{-C}_6\text{H}_5\text{F})][\text{BAR}^{\text{F}}_4]$ $J(\text{RhH}) = 59$ Hz.²⁵ Two distinct resonances are observed for the N–Me groups demonstrating a lack of rotation around the B–N bond on the NMR timescale, consistent with a B=N multiple bond character. The phenyl region shows 3 signals in the ratio 1 : 3 : 1 (in addition to the $[\text{BAR}^{\text{F}}_4]^-$ resonances), demonstrating that there is not free rotation around B(1)–C(1).

A plausible mechanism for the formation of complex (**11**) invokes dehydrogenation of (**II**) to form (**10**) and aminoborane (**6**), followed by much faster reaction of the latter with residual $[\text{Rh}(\text{P}^i\text{Pr}_3)_2(\eta^6\text{-C}_6\text{H}_5\text{F})][\text{BAR}^{\text{F}}_4]$ to form (**11**), overall in equal ratio to (**10**). When three equivalents of (**II**) were combined with $[\text{Rh}(\text{P}^i\text{Pr}_3)_2(\eta^6\text{-C}_6\text{H}_5\text{F})][\text{BAR}^{\text{F}}_4]$ the rapid (15 minutes) formation of only (**10**) was observed followed by the slow dehydrocoupling (hours) to form aminoborane (**6**), during which time (**10**) is observed as a resting state (Scheme 8). From this reaction mixture (**10**) could be isolated pure in good yield (57%) by layering with pentane and storage at –25 °C. A solution of pure (**10**) did not show any changes, suggesting (**11**) does not form from (**10**). Using aminoborane (**6**) generated catalytically (Scheme 6) reaction (overall oxidative addition) with $[\text{Rh}(\text{P}^i\text{Pr}_3)_2(\eta^6\text{-C}_6\text{H}_5\text{F})][\text{BAR}^{\text{F}}_4]$ is very rapid (on time of mixing) to form (**11**). In contrast there is no reaction of (**6**) with the Rh(I) sigma-complex (**1**) over 24 h, showing that aminoborane (**6**) will not displace amine–borane (**I**) under these conditions. A proposed mechanism is summarised in Scheme 9.

Complex (**11**) reacts with 2 equivalents of amine–borane (**II**) to give (**10**) and (**6**) on time of mixing. The current data do not discriminate between two possible mechanisms for this transformation. A sigma-bond metathesis/ β -elimination of (**11**) with (**II**) to eliminate (**6**), or a reversible reductive elimination of (**6**) to give a $\{\text{Rh}(\text{P}^i\text{Pr}_3)_2\}^+$ fragment which undergoes reaction with

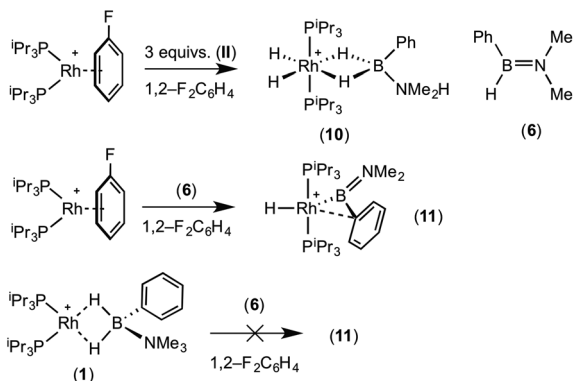


Scheme 9 Proposed mechanism for the formation of (**10**) and (**11**), and reactivity of (**11**) with amine–borane (**II**).

(**II**) as described (Scheme 8). Whatever the mechanism, complex (**10**) and aminoborane (**6**) are the ultimate products when excess amine–borane is present, consistent with their observation during catalysis. Pure complex (**10**) was found to be a slow catalyst for the dehydrogenation of (**II**) to form (**6**). Slow amine–borane dehydrogenation when catalysts sit in a Rh(III) dihydride resting state has been noted previously.^{35b}

Conclusions

We have shown here that the bite angle in $\{\text{Rh}(\text{P}_2)\}^+$ type fragments can have a significant effect in determining whether $\text{Rh}\cdots\text{H}_2\text{B}\eta^2$ -sigma amine–borane complexes or $\text{Rh}\cdots\text{arene}\eta^6$ complexes are formed with *B*-substituted amine–boranes. Wider bite angles (i.e. monodentate phosphines) tend to favour η^2 coordination modes, and relatively rapid B–H/N–H activation with a secondary *B*-substituted amine–borane to afford a Rh(III) dihydride complex and a *B*-substituted aminoborane. With constrained, chelating, phosphines η^6 complexes can be isolated instead in which the amine–borane moiety is intact and dehydrogenation is slow. This difference in stoichiometric reactivity balances out the reported large differences in catalytic dehydrocoupling rate of $\{\text{Rh}(\text{PR}_3)_2(\text{H})_2\}^+$ fragment (slow) versus $\{\text{Rh}(\text{chelating phosphine})\}^+$ (fast) with $\text{H}_3\text{B}\cdot\text{NMe}_2\text{H}$, which does not bear aryl substituents. Thus, although $\{\text{Rh}(\text{P}^i\text{Pr}_3)_2(\text{H})_2\}^+$ dehydrocouples $\text{H}_2\text{PhB}\cdot\text{NMe}_2\text{H}$ slowly, the η^6 coordination mode observed with $\{\text{Rh}(\text{P}^i\text{Pr}_2\text{P}(\text{CH}_2)_3\text{P}^i\text{Pr}_2)\}^+$ means that B–H (and subsequent N–H) activation by an inner sphere coordination/activation mechanism are also slowed so that now both fragments operate at a similar rate. Such observations are potentially important in the design of systems that dehydropolymerise arene-substituted amine–boranes (i.e. BN polystyrene analogues) as rapid dehydrogenation to form putative aminoborane intermediates that then can undergo B–N bond forming process are likely central to any successful catalyst system. We thus suggest that



Scheme 8 Reactivity of (**II**) and (**6**).



systems that form strong adducts with arene π -systems are less likely to be good candidates for such transformations.

Experimental

General experimental details

All manipulations, unless otherwise stated, were performed under an atmosphere of argon, using standard Schlenk and glove-box techniques. Glassware was oven dried at 130 °C overnight and flamed under vacuum prior to use. Dichloromethane, diethyl ether and pentane were dried using a Grubbs type solvent purification system (MBraun SPS-800) and degassed by successive freeze-pump-thaw cycles.⁴⁶ CD_2Cl_2 and 1,2- $\text{F}_2\text{C}_6\text{H}_4$ were distilled under vacuum from CaH_2 and stored over 3 Å molecular sieves, 1,2- $\text{F}_2\text{C}_6\text{H}_4$ was stirred over alumina for two hours prior to drying. NMR spectra were recorded on a Bruker AVD 500 MHz spectrometer at room temperature unless otherwise stated. For NMR spectra measured *in situ* in 1,2- $\text{F}_2\text{C}_6\text{H}_4$, the spectrometer was pre-locked and pre-shimmed using a C_6D_6 (0.1 mL) and 1,2- $\text{F}_2\text{C}_6\text{H}_4$ (0.3 mL) sample and ^1H NMR spectra were referenced to the centre of the downfield solvent multiplet (δ 7.07). ^{31}P and ^{11}B NMR spectra were referenced against 85% H_3PO_4 (external) and $\text{Et}_2\text{O}\cdot\text{BF}_3$ (external) respectively. Chemical shifts are quoted in ppm and coupling constants in Hz. ESI-MS were recorded on a Bruker MicroTOF instrument. In all ESI-MS spectra there was a good fit to both the principal molecular ion and the overall isotopic distribution. Microanalyses were performed by Stephen Boyer at the London Metropolitan University.

Metal precursor compounds $[\text{Rh}(\text{P}^i\text{Pr}_3)_2(\text{C}_6\text{H}_5\text{F})][\text{BAR}^{\text{F}}_4]$,²⁴ $[\text{Rh}(\text{P}^i\text{Bu}_3)_2(\text{C}_6\text{H}_5\text{F})][\text{BAR}^{\text{F}}_4]$,²⁵ $[\text{Rh}(\text{P}^i\text{Pr}_2\text{P}(\text{CH}_2)_3\text{P}^i\text{Pr}_2)(\text{C}_6\text{H}_5\text{F})][\text{BAR}^{\text{F}}_4]$,^{18b} $[\text{Rh}(\text{Ph}_2\text{P}(\text{CH}_2)_3\text{PPh}_2)(\text{C}_6\text{H}_5\text{F})][\text{BAR}^{\text{F}}_4]$ ^{17b} and $[\text{Rh}(\text{Ph}_2\text{P}(\text{CH}_2)_5\text{PPh}_2)(\text{C}_6\text{H}_5\text{F})][\text{BAR}^{\text{F}}_4]$ ^{17b} were prepared by literature methods and all other starting materials were used as received.

$\text{PhH}_2\text{B}\cdot\text{NMe}_3$ (I) and $\text{PhH}_2\text{B}\cdot\text{NMe}_2\text{H}$ (II)

$\text{Li}[\text{PhBH}_3]$ was prepared from $\text{PhB}(\text{OH})_2$ and $\text{Li}[\text{AlH}_4]$ as reported in the literature.²³ In a typical synthesis, $\text{Li}[\text{PhBH}_3]$ (350 mg, 3.57 mmol) and the appropriate ammonium chloride salt, $[\text{NMe}_3\text{H}]\text{Cl}$ (291 mg, 3.57 mmol) or $[\text{NMe}_2\text{H}_2]\text{Cl}$ (341 mg, 3.57 mmol) were added to a Schlenk flask and immediately dissolved in diethyl ether (20 mL). The mixture (a suspension of white solid) was stirred vigorously for 2 hours and evolution of hydrogen was observed. The mixture was evaporated to dryness *in vacuo* and pentane (100 mL) added and the mixture stirred vigorously. The solution was transferred by filter cannula to another Schlenk and the remaining white solid washed with pentane (2×10 mL). The combined fractions were evaporated to dryness *in vacuo* to yield the amine-borane $\text{PhH}_2\text{B}\cdot\text{NMe}_3$ (309 mg, 58%) or $\text{PhH}_2\text{B}\cdot\text{NMe}_2\text{H}$ (340 mg, 64%) as white solids which were stored in the glove box.

Both compounds have been reported previously although prepared by slightly different synthetic routes. The synthesis of

$\text{PhH}_2\text{B}\cdot\text{NMe}_3$ has been reported several times^{12,13,22,47} and NMR spectroscopy data have been reported in C_6D_6 .¹³ Our data for $\text{PhH}_2\text{B}\cdot\text{NMe}_3$ matched that previously reported. The synthesis of $\text{PhH}_2\text{B}\cdot\text{NMe}_2\text{H}$ has been reported by a different route¹⁴ but no NMR data was given and so is reported below for the first time.

$\text{PhH}_2\text{B}\cdot\text{NMe}_2\text{H}$ (II): ^1H NMR (400 MHz, CD_2Cl_2): δ 7.38 (apparent d, $^3J_{\text{HH}} = 6.9$ Hz, 2H, PhH), 7.21 (apparent t, $^3J_{\text{HH}} = 7.4$ Hz, 2H, PhH), 7.12 (apparent t, $^3J_{\text{HH}} = 7.4$ Hz, 1H, PhH), 3.52 (br, 1H, NH), 2.50 (s, 3H, NMe), 2.49 (s, 3H, NMe), 2.34 (br, 2H, BH_2). **$^{11}\text{B}\{^1\text{H}\}$ NMR (128.4 MHz, CD_2Cl_2):** δ -4.7 (s). **^{11}B NMR (128.4 MHz, CD_2Cl_2):** δ -4.7 (t, $J_{\text{BH}} = 97$ Hz). **$^{13}\text{C}\{^1\text{H}\}$ NMR (100.62 MHz, CD_2Cl_2):** δ 149.0 (br, *C-*ipso**), 135.6 (s, Ar), 127.3 (s, Ar), 127.3 (s, Ar), 125.4 (s, Ar), 42.2 (s, NMe).

Synthesis of metal complexes

$[\text{Rh}(\text{P}^i\text{Pr}_3)_2(\eta^2\text{-H}_2\text{PhB}\cdot\text{NMe}_3)][\text{BAR}^{\text{F}}_4]$ (1). To a Schlenk flask charged with $[\text{Rh}(\text{P}^i\text{Pr}_3)_2(\text{C}_6\text{H}_5\text{F})][\text{BAR}^{\text{F}}_4]$ (25.0 mg, 1.8×10^{-2} mmol) and $\text{PhH}_2\text{B}\cdot\text{NMe}_3$ (4 mg, 2.7×10^{-2} mmol, 1.5 equivalents) was added 1,2- $\text{F}_2\text{C}_6\text{H}_4$ (0.5 mL). The resulting blue/purple solution was layered with pentane at -25 °C to afford the product as blue crystals. Yield: 18 mg, 69%. **^1H NMR (500 MHz, CD_2Cl_2):** δ 7.76 (s, 8H, $[\text{BAR}^{\text{F}}_4]^-$), 7.60 (s, 4H, $[\text{BAR}^{\text{F}}_4]^-$), 7.37 (br, 3H, PhH), 7.25 (br, 2H, PhH), 2.83 (s, 9H, NMe_3), 2.07 (broad m, 6H, CH), 1.32 (apparent dd, $J \sim 12$, $J \sim 7$, 36H, CH_3 Hz), -6.36 (br, 2H, BH_2). **$^{31}\text{P}\{^1\text{H}\}$ NMR (202 MHz, CD_2Cl_2):** δ 69.6 (d, $J_{\text{RhP}} = 176$ Hz). **$^{11}\text{B}\{^1\text{H}\}$ NMR (160 MHz, CD_2Cl_2):** δ 34.8 (br, BH_2), -6.6 (s, $[\text{BAR}^{\text{F}}_4]^-$). **^{11}B NMR (160 MHz, CD_2Cl_2):** δ 34.8 (br, BH_2), -6.6 (s, $[\text{BAR}^{\text{F}}_4]^-$). **ESI-MS** (1,2- $\text{F}_2\text{C}_6\text{H}_4$, 60 °C) positive ion: m/z 572.32 $[\text{M}^+]$ (calc. 572.32). **Elemental microanalysis:** Calc. $[\text{C}_{59}\text{H}_{70}\text{B}_2\text{F}_{24}\text{NP}_2\text{Rh}]$ (1435.38 g mol⁻¹): C, 49.35; H, 4.91; N, 0.98. Found: C, 49.32; H, 4.82; N, 1.01.

$[\text{Rh}(\text{P}^i\text{Pr}_2\text{P}(\text{CH}_2)_3\text{P}^i\text{Pr}_2)(\eta^6\text{-PhH}_2\text{B}\cdot\text{NMe}_3)][\text{BAR}^{\text{F}}_4]$ (2). To a Schlenk flask charged with $[\text{Rh}(\text{P}^i\text{Pr}_2\text{P}(\text{CH}_2)_3\text{P}^i\text{Pr}_2)(\text{C}_6\text{H}_5\text{F})][\text{BAR}^{\text{F}}_4]$ (25.0 mg, 1.9×10^{-2} mmol) and $\text{PhH}_2\text{B}\cdot\text{NMe}_3$ (3.1 mg, 2.1×10^{-2} mmol, 1.1 equivalents) was added 1,2- $\text{F}_2\text{C}_6\text{H}_4$ (0.5 mL). Resulting orange solution was stirred for 30 minutes and layered with pentane at -25 °C to afford the product as orange crystals. Yield: 20.0 mg, 77%. **^1H NMR (500 MHz, CD_2Cl_2):** δ 7.76 (s, 8H, $[\text{BAR}^{\text{F}}_4]^-$), 7.60 (s, 4H, $[\text{BAR}^{\text{F}}_4]^-$), 6.93 (broad m, 1H, PhH), 6.31 (broad m, 4H, PhH), 2.55 (s, 9H, NMe_3), 1.88 (br, 6H, CH_2), 1.30 (br, 4H, CH), 1.19 (broad m, 12 H, CH_3), 1.12 (broad m, 12 H, CH_3), BH_2 signals not detected due to quadrupolar broadening. On ^{11}B decoupling BH_2 resonance appears at δ 2.38 (s). **$^{31}\text{P}\{^1\text{H}\}$ NMR (202 MHz, CD_2Cl_2):** δ 45.0 (d, $J_{\text{RhP}} = 195$ Hz). **$^{11}\text{B}\{^1\text{H}\}$ NMR (160 MHz, CD_2Cl_2):** δ -2.1 (br, BH_2), -6.6 (s, $[\text{BAR}^{\text{F}}_4]^-$). **^{11}B NMR (160 MHz, CD_2Cl_2):** δ -2.1 (br, BH_2), -6.6 (s, $[\text{BAR}^{\text{F}}_4]^-$). **ESI-MS** (1,2- $\text{F}_2\text{C}_6\text{H}_4$, 60 °C) positive ion: m/z 528.26 $[\text{M}^+]$ (calc. 528.26). **Elemental microanalysis:** Calc. $[\text{C}_{56}\text{H}_{62}\text{B}_2\text{F}_{24}\text{NP}_2\text{Rh}]$ (1391.32 g mol⁻¹): C, 48.32; H, 4.49; N, 1.01. Found: C, 48.19; H, 4.38; N, 0.92.

$[\text{Rh}(\text{P}^i\text{Bu}_3)_2(\eta^2\text{-H}_2\text{PhB}\cdot\text{NMe}_3)][\text{BAR}^{\text{F}}_4]$ (η^2 -3) and $[\text{Rh}(\text{P}^i\text{Bu}_3)_2(\eta^6\text{-PhH}_2\text{B}\cdot\text{NMe}_3)][\text{BAR}^{\text{F}}_4]$ (η^6 -3). To a Young's NMR tube charged with $[\text{Rh}(\text{P}^i\text{Bu}_3)_2(\text{C}_6\text{H}_5\text{F})][\text{BAR}^{\text{F}}_4]$ (10 mg, 6.82×10^{-3}



mmol) and $\text{PhH}_2\text{B}\cdot\text{NMe}_3$ (1.0 mg, 6.82×10^{-3} mmol, 1.0 equivalents) was added 1,2- $\text{F}_2\text{C}_6\text{H}_4$ (0.4 mL). Mixing resulted in blue/purple solution and NMR spectra were taken of this sample *in situ* to show products $\eta^2\text{-3}$ and $\eta^6\text{-3}$ in approximately equal ratio (see main text). The solvent from this sample was removed *in vacuo* and CD_2Cl_2 added and the NMR spectroscopy repeated to reveal virtually identical data in CD_2Cl_2 and this is reported below. Bulk isolation of either $\eta^2\text{-3}$ or $\eta^6\text{-3}$ was not possible due to formation of a mixture of purple crystals (determined by single crystal X-ray diffraction to be $\eta^2\text{-3}$) and an orange oil therefore microanalysis of the sample was not possible. ^1H NMR (500 MHz, CD_2Cl_2): δ 7.72 (s, 8H, $[\text{Bar}^{\text{F}}_4]^-$), 7.56 (s, 4H, $[\text{Bar}^{\text{F}}_4]^-$), 7.33 (broad m, \sim 1H, PhH, $\eta^2\text{-3}$), 7.18 (broad m, \sim 0.5H, PhH, $\eta^2\text{-3}$), 7.12 (broad m, \sim 1H, PhH, $\eta^2\text{-3}$), 6.95 (broad m, \sim 0.5H, PhH, $\eta^6\text{-3}$), 6.10 (broad m, \sim 1H, PhH, $\eta^6\text{-3}$), 5.94 (broad m, \sim 1H, PhH, $\eta^6\text{-3}$), 2.76 (s, \sim 4.5H, NMe_3 , $\eta^2\text{-3}$), 2.50 (s, \sim 4.5H, NMe_3 , $\eta^6\text{-3}$), 1.98 (broad m, 6H, CH), 1.63 (broad m, \sim 6H, CH_2), 1.55 (broad m, \sim 6H, CH_2), 1.06 (apparent broad d, $J \sim 5$ Hz, 36H, CH_3), -5.06 (br, \sim 1H, BH_2 , $\eta^2\text{-3}$). The signal for BH_2 in $\eta^6\text{-3}$ was not observed due to quadrupolar broadening and overlap with other resonances. A $^1\text{H}\{^{11}\text{B}\}$ NMR spectrum showed this peak at δ 2.41. $^{31}\text{P}\{^1\text{H}\}$ NMR (202 MHz, CD_2Cl_2): δ 34.1 (d, $J_{\text{PRh}} = 177$ Hz, $\eta^2\text{-3}$), 25.2 (d, $J_{\text{PRh}} = 202$ Hz, $\eta^6\text{-3}$). $^{11}\text{B}\{^1\text{H}\}$ NMR (160 MHz, CD_2Cl_2): δ 29.5 (br, BH_2 , $\eta^2\text{-3}$), -2.1 (br, BH_2 , $\eta^6\text{-3}$), -6.61 (s, $[\text{Bar}^{\text{F}}_4]^-$). ESI-MS (1,2- $\text{F}_2\text{C}_6\text{H}_4$, 60 °C) positive ion: m/z 656.41 $[\text{M}^+]$ (calc. 656.42).

$[\text{Rh}(\text{Ph}_2\text{P}(\text{CH}_2)_5\text{PPh}_2)(\eta^6\text{-PhH}_2\text{B}\cdot\text{NMe}_3)][\text{Bar}^{\text{F}}_4]$ (4). To a Schlenk flask charged with $[\text{Rh}(\text{Ph}_2\text{P}(\text{CH}_2)_5\text{PPh}_2)(\text{C}_6\text{H}_5\text{F})][\text{Bar}^{\text{F}}_4]$ (15.0 mg, 9.98×10^{-3} mmol) and $\text{PhH}_2\text{B}\cdot\text{NMe}_3$ (1.5 mg, 9.98×10^{-3} mmol, 1 equivalent) was added 1,2- $\text{F}_2\text{C}_6\text{H}_4$ (1.0 mL). The resulting orange solution was stirred for 30 minutes. The solvent was removed *in vacuo* and the orange oily solid redissolved in CH_2Cl_2 (1 mL). This solution was layered with pentane at -25 °C to afford the product as dark orange crystals. Yield: 5.0 mg, 32%. ^1H NMR (500 MHz, CD_2Cl_2): δ 7.72 (s, 8H, $[\text{Bar}^{\text{F}}_4]^-$), 7.56 (s, 4H, $[\text{Bar}^{\text{F}}_4]^-$), 7.41–7.31 (broad overlapping m, 20H, PhH), 7.12 (apparent broad t, $J_{\text{HH}} \sim 5.5$ Hz, 1H, PhH), 5.21–5.17 (broad overlapping m, 4H, PhH), 2.47 (broad m, overlap with 2.45 signal, 2H, CH_2), 2.45 (s, 9H, NMe_3), 2.30 (broad m, 4H, CH_2), 1.91 (broad m, 4H, CH_2). The signal for BH_2 in 4 was not observed due to quadrupolar broadening and overlap with other resonances. A $^1\text{H}\{^{11}\text{B}\}$ NMR spectrum showed this peak at δ 2.51. $^{31}\text{P}\{^1\text{H}\}$ NMR (202 MHz, CD_2Cl_2): δ 26.3 (d, $J_{\text{RHP}} = 204$ Hz). $^{11}\text{B}\{^1\text{H}\}$ NMR (160 MHz, CD_2Cl_2): δ -2.2 (br, BH_2), -6.6 (s, $[\text{Bar}^{\text{F}}_4]^-$). ^{11}B NMR (160 MHz, CD_2Cl_2): δ -2.2 (br, BH_2), -6.6 (s, $[\text{Bar}^{\text{F}}_4]^-$). ESI-MS (1,2- $\text{F}_2\text{C}_6\text{H}_4$, 60 °C) positive ion: m/z 692.22 $[\text{M}^+]$ (calc. 692.23). Elemental microanalysis: Calc. $[\text{C}_{70}\text{H}_{58}\text{B}_2\text{F}_{24}\text{NP}_2\text{Rh}]$ (1556.04 g mol $^{-1}$): C, 54.03; H, 3.76; N, 0.90. Found: C, 53.92; H, 3.67; N, 1.00.

$[\text{Rh}(\text{Ph}_2\text{P}(\text{CH}_2)_3\text{PPh}_2)(\eta^6\text{-PhH}_2\text{B}\cdot\text{NMe}_3)][\text{Bar}^{\text{F}}_4]$ (5). To a Schlenk flask charged with $[\text{Rh}(\text{Ph}_2\text{P}(\text{CH}_2)_3\text{PPh}_2)(\text{C}_6\text{H}_5\text{F})][\text{Bar}^{\text{F}}_4]$ (30.0 mg, 2.04×10^{-2} mmol) and $\text{PhH}_2\text{B}\cdot\text{NMe}_3$ (3.0 mg, 2.04×10^{-2} mmol, 1 equivalent) was added 1,2- $\text{F}_2\text{C}_6\text{H}_4$ (1.0 mL). The resulting orange solution was stirred for

30 minutes and layered with pentane at -25 °C to afford the product as orange crystals. Yield: 15.0 mg, 48%. ^1H NMR (500 MHz, CD_2Cl_2): δ 7.72 (s, 8H, $[\text{Bar}^{\text{F}}_4]^-$), 7.56 (s, 4H, $[\text{Bar}^{\text{F}}_4]^-$), 7.46 (broad m, 10H, PhH), 7.41–7.36 (broad m, 10H, PhH), 6.82 (apparent t, $^3J_{\text{HH}} = 6.1$ Hz, 1H, PhH), 5.55 (apparent d, $^3J_{\text{HH}} = 6.1$ Hz, 2H, PhH), 4.94 (apparent t, $^3J_{\text{HH}} = 6.1$ Hz, 2H, PhH), 2.48 (s, 9H, NMe_3), 2.45 (broad m, overlap with 2.48 signal, 4H, CH_2), 1.85 (broad m, 2H, CH_2). The signal for BH_2 in 5 was not observed due to quadrupolar broadening and overlap with other resonances. A $^1\text{H}\{^{11}\text{B}\}$ NMR spectrum showed this peak at δ 2.59. $^{31}\text{P}\{^1\text{H}\}$ NMR (202 MHz, CD_2Cl_2): δ 25.5 (d, $J_{\text{RHP}} = 192$ Hz). $^{11}\text{B}\{^1\text{H}\}$ NMR (160 MHz, CD_2Cl_2): δ -2.0 (br, BH_2), -6.6 (s, $[\text{Bar}^{\text{F}}_4]^-$). ^{11}B NMR (160 MHz, CD_2Cl_2): δ -2.0 (br, BH_2), -6.6 (s, $[\text{Bar}^{\text{F}}_4]^-$). ESI-MS (1,2- $\text{F}_2\text{C}_6\text{H}_4$, 60 °C) positive ion: m/z 664.19 $[\text{M}^+]$ (calc. 664.19). Elemental microanalysis: Calc. $[\text{C}_{68}\text{H}_{54}\text{B}_2\text{F}_{24}\text{NP}_2\text{Rh}]$ (1527.99 g mol $^{-1}$): C, 53.45; H, 3.56; N, 0.92. Found: C, 53.38; H, 3.43; N, 0.97.

$[\text{Rh}(\text{Pr}_2\text{P}(\text{CH}_2)_3\text{P}^i\text{Pr}_2)(\eta^6\text{-PhH}_2\text{B}\cdot\text{NMe}_2\text{H})][\text{Bar}^{\text{F}}_4]$ (7). To a Schlenk flask charged with $[\text{Rh}(\text{Pr}_2\text{P}(\text{CH}_2)_3\text{P}^i\text{Pr}_2)(\text{C}_6\text{H}_5\text{F})][\text{Bar}^{\text{F}}_4]$ (25.0 mg, 1.9×10^{-2} mmol) and $\text{PhH}_2\text{B}\cdot\text{NMe}_2\text{H}$ (2.8 mg, 2.1×10^{-2} mmol, 1.1 equivalents) was added 1,2- $\text{F}_2\text{C}_6\text{H}_4$ (0.5 mL). Resulting orange solution was stirred for 24 h and layered with pentane at -25 °C to afford the product as orange crystals. Yield: 16 mg, 62%. ^1H NMR (500 MHz, CD_2Cl_2): δ 7.76 (s, 8H, $[\text{Bar}^{\text{F}}_4]^-$), 7.60 (s, 4H, $[\text{Bar}^{\text{F}}_4]^-$), 6.88 (broad m, 1H, PhH), 6.31 (broad m, 2H, PhH), 6.26 (broad m, 2H, PhH), 3.55 (br, 1H, NH), 2.52 (s, 6H, NMe_2), 1.86 (br, 6H, CH_2), 1.30 (br, 4H, CH), 1.18 (broad m, 12, CH_3), 1.11 (broad m, 12, CH_3). BH_2 signals not detected due to quadrupolar broadening. $^{31}\text{P}\{^1\text{H}\}$ NMR (202 MHz, CD_2Cl_2): δ 45.3 (d, $J_{\text{RHP}} = 196$ Hz). $^{11}\text{B}\{^1\text{H}\}$ NMR (160 MHz, CD_2Cl_2): δ -6.0 (br, BH_2), -6.6 (s, $[\text{Bar}^{\text{F}}_4]^-$). ^{11}B NMR (160 MHz, CD_2Cl_2): δ -6.0 (br, BH_2), -6.6 (s, $[\text{Bar}^{\text{F}}_4]^-$). ESI-MS (1,2- $\text{F}_2\text{C}_6\text{H}_4$, 60 °C) positive ion: m/z 514.24 $[\text{M}^+]$ (calc. 514.25). Elemental microanalysis: Calc. $[\text{C}_{55}\text{H}_{60}\text{B}_2\text{F}_{24}\text{NP}_2\text{Rh}]$ (1377.31 g mol $^{-1}$): C, 47.96; H, 4.39; N, 1.02. Found: C, 47.60; H, 4.29; N, 1.13.

$[\text{Rh}(\text{Ph}_2\text{P}(\text{CH}_2)_3\text{Ph}_2)(\eta^6\text{-PhH}_2\text{B}\cdot\text{NMe}_2\text{H})][\text{Bar}^{\text{F}}_4]$ (8). To a Young's NMR tube charged with $[\text{Rh}(\text{Ph}_2\text{P}(\text{CH}_2)_3\text{PPh}_2)(\text{C}_6\text{H}_5\text{F})][\text{Bar}^{\text{F}}_4]$ (16.0 mg, 1.1×10^{-2} mmol) and $\text{PhH}_2\text{B}\cdot\text{NMe}_2\text{H}$ (1.5 mg, 1.1×10^{-2} mmol) was added 1,2- $\text{F}_2\text{C}_6\text{H}_4$ (0.5 mL). The resulting orange solution was left at room temperature for 10 minutes to form (8) which was *in situ* characterised by the NMR spectroscopy. ^1H NMR (500 MHz, 1,2- $\text{F}_2\text{C}_6\text{H}_4$): δ 8.34 (s, 8H, $[\text{Bar}^{\text{F}}_4]^-$), 7.70 (s, 4H, $[\text{Bar}^{\text{F}}_4]^-$), 5.68 (apparent d, $^3J_{\text{HH}} = 6.1$ Hz, 2H, PhH), 5.01 (apparent t, $^3J_{\text{HH}} = 6.1$ Hz, 2H, PhH), 2.79 (br, 1H, NH), 3.04–2.67 (br, 2H, BH_2), 2.48 (s, 6H, NMe_2), 2.40 (br, 4H, CH_2), 1.87 (broad m, 2H, CH_2). The remaining phenyl signals were obscured by the 1,2- $\text{F}_2\text{C}_6\text{H}_4$ signals. BH_2 signal was observed at δ 2.81 (s, 2H) in the $^1\text{H}\{^{11}\text{B}\}$ NMR spectrum. $^{31}\text{P}\{^1\text{H}\}$ NMR (202 MHz, 1,2- $\text{F}_2\text{C}_6\text{H}_4$): δ 25.2 (d, $J_{\text{RHP}} = 193$ Hz). $^{11}\text{B}\{^1\text{H}\}$ NMR (160 MHz, 1,2- $\text{F}_2\text{C}_6\text{H}_4$): δ -5.0 (br, BH_2), -6.6 (s, $[\text{Bar}^{\text{F}}_4]^-$).

$[\text{Rh}(\text{P}^i\text{Pr}_3)_2(\text{H})_2(\eta^2\text{-H}_2\text{PhB}\cdot\text{NMe}_2\text{H})][\text{Bar}^{\text{F}}_4]$ (10). To a sealed NMR tube charged with $[\text{Rh}(\text{P}^i\text{Pr}_3)_2(\text{C}_6\text{H}_5\text{F})][\text{Bar}^{\text{F}}_4]$ (25.0 mg, 1.8×10^{-2} mmol) and $\text{PhH}_2\text{B}\cdot\text{NMe}_2\text{H}$ (7.2 mg, 5.4×10^{-2}



mmol, 3 equivalents) was added 1,2-F₂C₆H₄ (0.5 mL). Resulting colourless solution was mixed by inversion for 15 minutes and then transferred to a crystallization tube. The 1,2-F₂C₆H₄ solution was layered with pentane and kept -25 °C for two days to afford the product as colourless crystals. Yield: 15 mg, 57%. ¹H NMR (500 MHz, CD₂Cl₂): δ 7.76 (s, 8H, [BAR^F₄]⁻), 7.60 (s, 4H, [BAR^F₄]⁻), 7.44 (broad m, 2H, PhH), 7.39 (broad m, 3H, PhH), 3.92 (s, 1H, NH), 2.64 (s, 6H, NMe₂), 1.90 (br, 6H, CH), 1.22 (apparent dd, *J* ~ 13, *J* ~ 6, 36H, CH₃), -2.08 (br, 2H, BH₂), -19.05 (broad m, 2H, RhH₂). ¹H{³¹P} NMR (500 MHz, CD₂Cl₂): δ 7.76 (s, 8H, [BAR^F₄]⁻), 7.60 (s, 4H, [BAR^F₄]⁻), 7.44 (broad m, 2H, PhH), 7.39 (broad m, 3H, PhH), 3.92 (s, 1H, NH), 2.64 (s, 6H, NMe₂), 1.90 (br, 6H, CH), 1.22 (broad d, *J* ~ 6, 36H, CH₃), -2.08 (br, 2H, BH₂), -19.05 (broad d, *J*_{RhH} = 17, 2H, RhH₂). ³¹P{¹H} NMR (202 MHz, CD₂Cl₂): δ 64.7 (d, *J*_{RhP} = 108 Hz). ¹¹B{¹H} NMR (160 MHz, CD₂Cl₂): δ 8.0 (br, BH₂), -6.6 (s, [BAR^F₄]⁻). ¹¹B NMR (160 MHz, CD₂Cl₂): δ 8.0 (br, BH₂), -6.6 (s, [BAR^F₄]⁻). ESI-MS (1,2-F₂C₆H₄, 60 °C) positive ion: *m/z* 560.32 [M⁺] (calc. 560.32). Elemental microanalysis: Calc. [C₅₈H₇₀B₂F₂₄NP₂Rh] (1435.38 g mol⁻¹): C, 48.93; H, 4.96; N, 0.98. Found: C, 48.96; H, 4.62; N, 0.98.

[Rh(PⁱPr₃)₂(H)(BPhNMe₂)] [BAR^F₄] (11). To a sealed NMR tube charged with [Rh(PⁱPr₃)₂(C₆H₅F)] [BAR^F₄] (25.0 mg, 1.8 × 10⁻² mmol) and PhH₂B-NMe₂H (2.4 mg, 1.8 × 10⁻² mmol) was added 1,2-F₂C₆H₄ (0.5 mL). Addition of 1,2-F₂C₆H₄ immediately resulted in a purple solution which turned to colourless in 5 minutes. Resulting colourless solution was mixed by inversion for 24 h which turned the colourless solution to yellow. The yellow solution was transferred to a crystallization tube, layered with pentane and kept -25 °C for two days which resulted in the formation of majority of pale yellow crystals and some colourless crystals. Pale yellow crystals were mechanically separated from the mixture for characterisation. Yield: 10 mg, 38%. ¹H NMR (500 MHz, CD₂Cl₂): δ 7.76 (s, 8H, [BAR^F₄]⁻), 7.67 (m, 1H, Ph), 7.60 (s, 4H, [BAR^F₄]⁻), 7.55 (broad d, 2H, Ph), 7.54 (br, 2H, PhH), 3.07 (s, 3H, NMe), 2.95 (s, 3H, NMe), 2.23 (br, 6H, CH), 1.26 (apparent dd, *J* ~ 13 Hz, *J* ~ 6 Hz, 18H, CH₃), 1.18 (apparent dd, *J* ~ 13 Hz, *J* ~ 6, 18H, CH₃), -21.71 (doublet of triplets, *J*_{RhH} = 64 Hz, *J*_{PH} = 12 Hz, 1H, RhH). The pale yellow solution of (11) in CD₂Cl₂ was not stable and decomposed in 6 h to form dark yellow solution of uncharacterised complexes. ¹H{³¹P} NMR (500 MHz, CD₂Cl₂, hydride region): δ -21.71 (d, *J*_{RhH} = 64 Hz, 1H, RhH). ³¹P{¹H} NMR (202 MHz, CD₂Cl₂): δ 48.8 (d, *J*_{RhP} = 120 Hz). ¹¹B{¹H} NMR (160 MHz, CD₂Cl₂): δ 50.1 (br, RhB), -6.6 (s, [BAR^F₄]⁻). ¹¹B NMR (160 MHz, CD₂Cl₂): δ 50.1 (br, RhB), -6.6 (s, [BAR^F₄]⁻). ¹³C{¹H} NMR (100.62 MHz, CD₂Cl₂): Shifts due to [BAR^F₄]⁻ anion: δ 161.7 (q, *J*_{BC} = 50 Hz), 134.8 (s), 128.8 (quartet of quartet, ²*J*_{FC} = 26 Hz, ³*J*_{BC} = 3 Hz), 124.6 (q, *J*_{FC} = 272 Hz), 117.4 (apparent septet, ³*J*_{FC} = 4 Hz); Shifts due to cation: δ 132.2 (s, Ph), 130.7 (s, Ph), 127.8 (s, Ph), 43.33 (s, NMe), 40.41 (s, NMe), 24.6 (overlapping doublets, *J*_{PC} = 12 Hz, CH_{3iPr}), 19.9 (s, CH_{3iPr}), 19.1 (s, CH_{3iPr}). ESI-MS (1,2-F₂C₆H₄, 60 °C) positive ion: *m/z* 556.29 [M⁺] (calc. 556.29). Elemental microanalysis: Calc. [C₅₈H₆₆B₂F₂₄NP₂Rh] (1419.35 g mol⁻¹): C, 49.07; H, 4.69; N, 0.99. Found: C, 49.45; H, 4.20; N, 0.75.

Catalytic generation of aminoborane PhHB=NMe₂ (6)

The aminoborane PhHB=NMe₂ (II) was generated catalytically by heating a mixture of amine-borane PhH₂B-NMe₂H (0.9 mg, 0.0070 mmol) and [Rh(PⁱPr₃)₂(C₆H₅F)] [BAR^F₄] (0.5 mg, 0.00035 mmol, 5 mol%) in 1,2-F₂C₆H₄ (0.35 mL) in a high pressure Young's tap NMR tube for 1 hour (77 °C). Attempts to isolate (6) from this mixture by vacuum distillation resulted in decomposition of the aminoborane to uncharacterised products however, we found this solution was sufficiently pure for further reaction. The NMR data reported was measured *in situ* in 1,2-F₂C₆H₄ after complete catalytic conversion. PhHB=NMe₂ (6): ¹H NMR (500 MHz, 1,2-F₂C₆H₄): δ 5.05 (broad q, *J*_{HB} = 120 Hz, 1H, BH), 3.02 (s, 3H, NMe), 2.88 (s, 3H, NMe), phenyl resonances were obscured due to the solvent (1,2-F₂C₆H₄) peaks. ¹¹B{¹H} NMR (160 MHz, 1,2-F₂C₆H₄): δ 39.4 (s). ¹¹B NMR (160 MHz, 1,2-F₂C₆H₄): δ 39.4 (d, ¹*J*_{BH} = 123 Hz).

Reaction of aminoborane (6) with sigma-complex (1)

PhHB=NMe₂ (6) was generated catalytically as above using PhH₂B-NMe₂H (0.9 mg, 0.0070 mmol) and [Rh(PⁱPr₃)₂(C₆H₅F)] [BAR^F₄] (0.5 mg, 0.00035 mmol, 5 mol%). Clean conversion to (6) was checked by ¹¹B NMR spectroscopy and this solution transferred *via* cannula to an NMR tube containing [Rh-(PⁱPr₃)₂(η²-H₂PhB-NMe₃)] [BAR^F₄] (1) (10.0 mg, 0.0070 mmol). The reaction was mixed and no colour change was observed. Immediate NMR spectroscopy showed no reaction between (6) and (1) and no change in these spectra was observed after 24 h mixing of the solution by inversion at room temperature.

Reaction of aminoborane (6) with [Rh(PⁱPr₃)₂(C₆H₅F)] [BAR^F₄] – an alternative synthesis of (11)

PhHB=NMe₂ (6) was generated catalytically as above using PhH₂B-NMe₂H (1.8 mg, 0.0133 mmol) and [Rh(PⁱPr₃)₂(C₆H₅F)] [BAR^F₄] (0.9 mg, 0.00067 mmol, 5 mol%). Clean conversion to (6) was checked by ¹¹B NMR spectroscopy and this solution transferred *via* cannula to an NMR tube containing [Rh(PⁱPr₃)₂(η⁶-C₆H₅F)] [BAR^F₄] (18.4 mg, 0.0133 mmol). The solution was mixed and immediate NMR spectroscopy showed almost quantitative conversion (>95%) to (11) with NMR spectra (measured *in situ* in 1,2-F₂C₆H₄) matching those reported above. Crystallisation of this solution by layering with pentane and storage at -18 °C resulted in formation of crystals of (11).

Acknowledgements

The EPSRC (EP/J02127X) and the Rhodes Trust for funding.

Notes and references

- (a) C. W. Hamilton, R. T. Baker, A. Staubitz and I. Manners, *Chem. Soc. Rev.*, 2009, **38**, 279–293; (b) A. Staubitz, A. P. M. Robertson and I. Manners, *Chem. Rev.*, 2010, **110**, 4079–4124.



- 2 (a) E. M. Leitao, T. Jurca and I. Manners, *Nat. Chem.*, 2013, **5**, 817–829; (b) R. Waterman, *Chem. Soc. Rev.*, 2013, **42**, 5629–5641.
- 3 H. C. Johnson, T. N. Hooper and A. S. Weller, in *Synthesis and Application of Organoboron Compounds, Topics in Organometallic Chemistry*, ed. E. Fernández and A. Whiting, Springer International Publishing, 2015, vol. 49, pp. 153–220.
- 4 A. Staubitz, A. P. M. Robertson, M. E. Sloan and I. Manners, *Chem. Rev.*, 2010, **110**, 4023–4078.
- 5 (a) C. A. Jaska, K. Temple, A. J. Lough and I. Manners, *J. Am. Chem. Soc.*, 2003, **125**, 9424–9434; (b) H. Helten, A. P. M. Robertson, A. Staubitz, J. R. Vance, M. F. Haddow and I. Manners, *Chem. – Eur. J.*, 2012, **18**, 4665–4680; (c) S.-K. Kim, S.-A. Hong, H.-J. Son, W.-S. Han, A. Michalak, S.-J. Hwang and S. O. Kang, *Dalton Trans.*, 2015, **44**, 7373–7381.
- 6 (a) M. Shimoi, S.-i. Nagai, M. Ichikawa, Y. Kawano, K. Katoh, M. Uruichi and H. Ogino, *J. Am. Chem. Soc.*, 1999, **121**, 11704–11712; (b) G. J. Kubas, *Metal Dihydrogen and σ -Bond Complexes*, Springer, New York, 2001; (c) G. Alcaraz and S. Sabo-Etienne, *Angew. Chem., Int. Ed.*, 2010, **49**, 7170–7179.
- 7 (a) P. G. Campbell, J. S. A. Ishibashi, L. N. Zakharov and S.-Y. Liu, *Aust. J. Chem.*, 2014, **67**, 521–524; (b) N. E. Stubbs, A. Schäfer, A. P. M. Robertson, E. M. Leitao, T. Jurca, H. A. Sparkes, C. H. Woodall, M. F. Haddow and I. Manners, *Inorg. Chem.*, 2015, **54**, 10878–10889.
- 8 (a) H. Anane, A. Jarid, A. Boutalib, I. Nebot-Gil and F. Tomás, *J. Mol. Struct. (THEOCHEM)*, 1998, **455**, 51–57; (b) D. J. Grant, M. H. Matus, K. D. Anderson, D. M. Camaioni, S. R. Neufeldt, C. F. Lane and D. A. Dixon, *J. Phys. Chem. A*, 2009, **113**, 6121–6132.
- 9 (a) A. P. M. Robertson, G. R. Whittell, A. Staubitz, K. Lee, A. J. Lough and I. Manners, *Eur. J. Inorg. Chem.*, 2011, **2011**, 5279–5287; (b) A. P. M. Robertson, M. F. Haddow and I. Manners, *Inorg. Chem.*, 2012, **51**, 8254–8264.
- 10 P. G. Campbell, A. J. V. Marwitz and S.-Y. Liu, *Angew. Chem., Int. Ed.*, 2012, **51**, 6074–6092.
- 11 (a) P. G. Campbell, L. N. Zakharov, D. J. Grant, D. A. Dixon and S.-Y. Liu, *J. Am. Chem. Soc.*, 2010, **132**, 3289–3291; (b) W. Luo, L. N. Zakharov and S.-Y. Liu, *J. Am. Chem. Soc.*, 2011, **133**, 13006–13009; (c) W. Luo, P. G. Campbell, L. N. Zakharov and S.-Y. Liu, *J. Am. Chem. Soc.*, 2011, **133**, 19326–19329; (d) W. Luo, D. Neiner, A. Karkamkar, K. Parab, E. B. Garner III, D. A. Dixon, D. Matson, T. Autrey and S.-Y. Liu, *Dalton Trans.*, 2013, **42**, 611–614; (e) G. Chen, L. N. Zakharov, M. E. Bowden, A. J. Karkamkar, S. M. Whittemore, E. B. Garner, T. C. Mikulas, D. A. Dixon, T. Autrey and S.-Y. Liu, *J. Am. Chem. Soc.*, 2015, **137**, 134–137; (f) A. Kumar, J. S. A. Ishibashi, T. N. Hooper, T. C. Mikulas, D. A. Dixon, S.-Y. Liu and A. S. Weller, *Chem. – Eur. J.*, 2016, **22**, 310–322.
- 12 E. Wiberg, J. E. F. Evans and H. Noth, *Z. Naturforsch., B: Anorg. Chem. Org. Chem. Biochem. Biophys. Biol.*, 1958, **13**, 263–264.
- 13 Y. Kawano, K. Yamaguchi, S.-y. Miyake, T. Kakizawa and M. Shimoi, *Chem. – Eur. J.*, 2007, **13**, 6920–6931.
- 14 B. M. Mikhailov and V. A. Dorokhov, *Russ. Chem. Bull.*, 1962, **11**, 1138–1142.
- 15 S.-K. Kim, W.-S. Han, T.-J. Kim, T.-Y. Kim, S. W. Nam, M. Mitoraj, Ł. Piekoś, A. Michalak, S.-J. Hwang and S. O. Kang, *J. Am. Chem. Soc.*, 2010, **132**, 9954–9955.
- 16 (a) P. Dierkes and P. W. N. M. van Leeuwen, *J. Chem. Soc., Dalton Trans.*, 1999, 1519–1530; (b) D. Aguila, E. Escribano, S. Speed, D. Talancon, L. Yerman and S. Alvarez, *Dalton Trans.*, 2009, 6610–6625.
- 17 (a) A. B. Chaplin and A. S. Weller, *Inorg. Chem.*, 2010, **49**, 1111–1121; (b) R. Dallanegra, A. P. M. Robertson, A. B. Chaplin, I. Manners and A. S. Weller, *Chem. Commun.*, 2011, **47**, 3763–3765.
- 18 (a) S. D. Pike, I. Pernik, R. Theron, J. S. McIndoe and A. S. Weller, *J. Organomet. Chem.*, 2015, **784**, 75–83; (b) I. Pernik, J. F. Hooper, A. B. Chaplin, A. S. Weller and M. C. Willis, *ACS Catal.*, 2012, **2**, 2779–2786.
- 19 J. Silvestre and T. A. Albright, *J. Am. Chem. Soc.*, 1985, **107**, 6829–6841.
- 20 T. A. Albright, J. K. Burdett and M. H. Whangbo, *Orbital Interactions in Chemistry*, 2nd edn, Wiley, New York, 2013.
- 21 M.-D. Su and S.-Y. Chu, *Inorg. Chem.*, 1998, **37**, 3400–3406.
- 22 M. F. Hawthorne, *J. Am. Chem. Soc.*, 1958, **80**, 4291–4293.
- 23 B. Singaram, T. E. Cole and H. C. Brown, *Organometallics*, 1984, **3**, 774–777.
- 24 A. B. Chaplin, A. I. Poblador-Bahamonde, H. A. Sparkes, J. A. K. Howard, S. A. Macgregor and A. S. Weller, *Chem. Commun.*, 2009, 244–246.
- 25 T. M. Douglas, A. B. Chaplin and A. S. Weller, *Organometallics*, 2008, **27**, 2918–2921.
- 26 C. A. Tolman, *Chem. Rev.*, 1977, **77**, 313–348.
- 27 T. M. Douglas, A. B. Chaplin, A. S. Weller, X. Yang and M. B. Hall, *J. Am. Chem. Soc.*, 2009, **131**, 15440–15456.
- 28 N. Merle, G. Koicok-Köhn, M. F. Mahon, C. G. Frost, G. D. Ruggerio, A. S. Weller and M. C. Willis, *Dalton Trans.*, 2004, 3883–3892.
- 29 G. Alcaraz, E. Clot, U. Helmstedt, L. Vendier and S. Sabo-Etienne, *J. Am. Chem. Soc.*, 2007, **129**, 8704–8705.
- 30 (a) H. C. Johnson, C. L. McMullin, S. D. Pike, S. A. Macgregor and A. S. Weller, *Angew. Chem., Int. Ed.*, 2013, **52**, 9776–9780; (b) L. J. Sewell, A. B. Chaplin and A. S. Weller, *Dalton Trans.*, 2011, **40**, 7499–7501.
- 31 (a) P. Pregosin, *NMR in Organometallic Chemistry*, Wiley-VCH, Weinheim, 2012; (b) A. Woolf, A. B. Chaplin, J. E. McGrady, M. A. M. Alibadi, N. Rees, S. Draper, F. Murphy and A. S. Weller, *Eur. J. Inorg. Chem.*, 2011, **2011**, 1614–1625.
- 32 W. F. Bailey, H. Connon, E. L. Eliel and K. B. Wiberg, *J. Am. Chem. Soc.*, 1978, **100**, 2202–2209.
- 33 T. M. Douglas, E. Molinos, S. K. Brayshaw and A. S. Weller, *Organometallics*, 2007, **26**, 463–465.
- 34 (a) P. Herich, J. Kameníček, K. Kuča, M. Pohanka and M. Olšovský, *Polyhedron*, 2009, **28**, 3565–3569;



- (b) M. Schwach, H. D. Hausen and W. Kaim, *Chem. – Eur. J.*, 1996, **2**, 446–451.
- 35 (a) A. D. Wilson, A. J. M. Miller, D. L. DuBois, J. A. Labinger and J. E. Bercaw, *Inorg. Chem.*, 2010, **49**, 3918–3926; (b) L. J. Sewell, G. C. Lloyd-Jones and A. S. Weller, *J. Am. Chem. Soc.*, 2012, **134**, 3598–3610.
- 36 (a) Y. Kawano, M. Uruichi, M. Shimoi, S. Taki, T. Kawaguchi, T. Kakizawa and H. Ogino, *J. Am. Chem. Soc.*, 2009, **131**, 14946–14957; (b) L. Pasumansky, D. Haddenham, J. W. Clary, G. B. Fisher, C. T. Goralski and B. Singaram, *J. Org. Chem.*, 2008, **73**, 1898–1905.
- 37 (a) R. Dallanegra, A. B. Chaplin and A. S. Weller, *Angew. Chem., Int. Ed.*, 2009, **48**, 6875–6878; (b) X. Chen, J.-C. Zhao and S. G. Shore, *Acc. Chem. Res.*, 2013, **46**, 2666–2675; (c) V. S. Nguyen, M. H. Matus, D. J. Grant, M. T. Nguyen and D. A. Dixon, *J. Phys. Chem. A*, 2007, **111**, 8844–8856; (d) A. Kumar, H. C. Johnson, T. N. Hooper, A. S. Weller, A. G. Algarra and S. A. Macgregor, *Chem. Sci.*, 2014, **5**, 2546–2553.
- 38 J. F. Hartwig, *Organotransition Metal Chemistry*, University Science Books, Sausalito, USA, 2010.
- 39 A. G. Algarra, L. J. Sewell, H. C. Johnson, S. A. Macgregor and A. S. Weller, *Dalton Trans.*, 2014, **43**, 11118–11128.
- 40 (a) C. Y. Tang, N. Phillips, J. I. Bates, A. L. Thompson, M. J. Gutmann and S. Aldridge, *Chem. Commun.*, 2012, **48**, 8096; (b) M. O'Neill, D. A. Addy, I. Riddlestone, M. Kelly, N. Phillips and S. Aldridge, *J. Am. Chem. Soc.*, 2011, **133**, 11500–11503; (c) C. Y. Tang, A. L. Thompson and S. Aldridge, *J. Am. Chem. Soc.*, 2010, **132**, 10578–10591.
- 41 H. C. Johnson, E. M. Leitao, G. R. Whittell, I. Manners, G. C. Lloyd-Jones and A. S. Weller, *J. Am. Chem. Soc.*, 2014, **136**, 9078–9093.
- 42 H. Braunschweig, R. D. Dewhurst and V. H. Gessner, *Chem. Soc. Rev.*, 2013, **42**, 3197–3208.
- 43 A. C. Cooper, E. Clot, J. C. Huffman, W. E. Streib, F. Maseras, O. Eisenstein and K. G. Caulton, *J. Am. Chem. Soc.*, 1999, **121**, 97–106.
- 44 N. H. Dryden, P. Legzdins, J. Trotter and V. C. Yee, *Organometallics*, 1991, **10**, 2857–2870.
- 45 (a) S. A. Westcott, N. J. Taylor, T. B. Marder, R. T. Baker, N. J. Jones and J. C. Calabrese, *J. Chem. Soc., Chem. Commun.*, 1991, 304–305; (b) W. H. Lam, S. Shimada, A. S. Batsanov, Z. Lin, T. B. Marder, J. A. Cowan, J. A. K. Howard, S. A. Mason and G. J. McIntyre, *Organometallics*, 2003, **22**, 4557–4568.
- 46 A. B. Pangborn, M. A. Giardello, R. H. Grubbs, R. K. Rosen and F. J. Timmers, *Organometallics*, 1996, **15**, 1518–1520.
- 47 J. J. Miller and F. A. Johnson, *Inorg. Chem.*, 1970, **9**, 69–74.

